

INVESTIGATING THE EFFECT OF RECHARGE ON INLAND FRESHWATER LENS
FORMATION AND DEGRADATION IN NORTHERN KUWAIT

by

RACHEL ROSE ROTZ

(Under the Direction of Adam Milewski)

ABSTRACT

Renewable freshwater resources in Kuwait exist as inland lenses and serve as an emergency resource in the northern Raudhatain and Umm Al-Aish basins. Recent studies suggest the inland lenses across the Arabian Peninsula are more numerous than believed. Specific geologic and hydrologic conditions are requisite for the formation and sustainability of these resources. Investigations into lens geometry as a function of recharge are needed to assess the amount of available freshwater. This study uses a physical model to examine differences between inland and oceanic island lens geometry (i.e. thickness, length), as well as the effect of recharge rate on lens formation and degradation. Results demonstrate inland lenses are thinner and longer than oceanic island lenses, are correlated to recharge rate, extend laterally, and degrade through time. The proper management and estimation of known reserves and development of new resources depend on understanding inland freshwater lens dynamics.

INDEX WORDS: Inland freshwater lenses, Kuwait, physical modeling, desert hydrology

INVESTIGATING THE EFFECT OF RECHARGE ON INLAND FRESHWATER LENS
FORMATION AND DEGRADATION IN NORTHERN KUWAIT

by

RACHEL ROSE ROTZ

BS, University of Georgia, 2014

BA, University of Central Florida, 1997

A Thesis Submitted to the Graduate Faculty of The University of Georgia in Partial Fulfillment
of the Requirements for the Degree

MASTER OF SCIENCE

ATHENS, GEORGIA

2016

© 2016

Rachel Rose Rotz

All Rights Reserved

INVESTIGATING THE EFFECT OF RECHARGE ON INLAND FRESHWATER LENS
FORMATION AND DEGRADATION IN NORTHERN KUWAIT

by

RACHEL ROSE ROTZ

Major Professor: Adam Milewski
Committee: Todd Rasmussen
Paul Schroeder

Electronic Version Approved:

Suzanne Barbour
Dean of the Graduate School
The University of Georgia
August 2016

ACKNOWLEDGEMENTS

Foremost, I offer my sincere gratitude to my advisor, Professor Milewski for the continuous support throughout my studies, for his guidance, enthusiasm, and unfettered cultivation of my understanding of water resources. In addition, I would like to thank my thesis committee: Professor Todd Rasmussen and Professor Paul Schroeder for their encouragement and insightful comments. My sincere thanks also go to Professor John Dowd for his immense knowledge and mentorship. I thank the Society of Exploration Geophysics for providing a scholarship to fund this project and Barq Albraq for permission to use the photographs in this document. Also, I thank my lab mates Seyoum Wondwosen, Khalil Lezzaik, Michael Durham, and Veronica Fay for their friendship and support. Lastly, I thank the love of my life, Cameron Brooks, for encouraging me to follow my heart.

TABLE OF CONTENTS

	Page
ACKNOWLEDGEMENTS	iv
LIST OF TABLES	vii
LIST OF FIGURES	viii
CHAPTER	
1 INTRODUCTION	1
2 SITE DESCRIPTION	6
2.1 Climate	6
2.2 Physiography	11
2.3 Geology and Aquifers	15
2.4 Hydrogeology and Water Quality	19
3 LITERATURE REVIEW	22
3.1 Climate Variability and Recharge in Kuwait	22
3.2 Lens Recharge	25
3.3 Geomorphic Analyses and Lens Locations	27
3.4 Oceanic Island and Inland Lenses	29
4 METHODS	32
4.1 Objectives	32
4.2 Physical Model	32
4.3 Simulations	38

4.4 Differences between Island and Inland Lenses.....	39
4.5 Recharge Rate on Lens Formation and Degradation	40
4.6 General Comments on the Physical Model.....	41
5 RESULTS AND DISCUSSION.....	42
5.1 Analytical and Observed Lenses Comparison	43
5.2 Recharge Effect on Observed Lens Formation.....	48
5.3 Recharge Effect on Degradation Rate.....	51
6 SUMMARY AND CONCLUSION	54
REFERENCES	60
APPENDICES	
A Appendix A: Lens Simulation Example	57
B Appendix B: Lens Thickness and Length Statistics	58
C Appendix C: Lens Thickness and Length Regressions.....	59

LIST OF TABLES

	Page
Table 1: Surface Sediment Hydraulic Conductivity Measurements.....	20
Table 2: Infiltration Rates of Northern Kuwait.....	21
Table 3: Kuwait City Aquifer Parameters	21
Table 4: Physical Model Salinity Measurements and Conversions.....	33
Table 5: Simulation Parameter Values	42
Table 6: Measured Simulation Values.....	45
Table 7: Time to Maximum Thickness Values.....	49
Table 8: Predicted Values of Lens Degradation	53

LIST OF FIGURES

	Page
Figure 1: Map of Arabian Peninsula Territories and Kuwait	8
Figure 2: Kuwait Elevation and Known Lenses	9
Figure 3: Temperature and Precipitation Values in Kuwait	10
Figure 4: Dust Fallout and Drought in Kuwait	10
Figure 5: Landforms in Kuwait.....	13
Figure 6: Elevation, salinity, and wadi networks of northern Kuwait	13
Figure 7: Example of saturated conditions in Kuwait	14
Figure 8: Regional Geology of Northern Kuwait	17
Figure 9: Cross-section of Northern Kuwait and Subah Ahmed National Reserve	18
Figure 10: Surface Topography of Kuwait Cross-section	20
Figure 11: SPI Index and Drought Characterization of Northern Kuwait	23
Figure 12: Sand Encroachment in Subah Ahmed National Reserve	24
Figure 13: Cross-section of Raudhatain Depression.....	26
Figure 14: Proposed Lens Locations and Um-Rimam Depression.....	28
Figure 15: Typical Oceanic Island Lens Schematic	31
Figure 16: Physical Model Conceptual Design	35
Figure 17: Physical Model and Components	36
Figure 18: Grain Size Analysis	36
Figure 19: Physical Model Setup Prior to Simulation	37

Figure 20: Simulation Parameters Schematic	41
Figure 21: Observed vs. Analytical Lens.....	43
Figure 22: Lens Thickness vs. Recharge Rate Including All Simulations	46
Figure 23: Lens Length vs. Recharge Rate Including All Simulations	46
Figure 24: Lens Thickness vs. Recharge Rate Including Without Large Recharge Areas	47
Figure 25: Lens Length vs. Recharge Rate Including Without Large Recharge Areas	47
Figure 26: Maximum Thickness Measurement Example	49
Figure 27: Time to Maximum Thickness vs. Recharge Rate	50
Figure 28: Lens Length and Thickness Regressions vs. Recharge Rate.....	50
Figure 29: Degradation Example	53
Figure 30: Prediction of Lens Degradation vs. Recharge Rate.....	53

CHAPTER 1

INTRODUCTION

Freshwater resources in arid environments are of great importance for drinking water, agriculture, and industrial use. Unfortunately, supply is often low to nonexistent, especially where groundwater is salty, precipitation is low, evaporation rates exceed precipitation, and surface water bodies are absent. Only after intense rainfall, runoff is produced and freshwater temporarily accumulates in wadi channels and topographic depressions. These ephemeral streams and ponds have supplied freshwater to the people of Kuwait in ancient times, but no longer support the country's increasing water demands. In the mid-twentieth century, Kuwait commissioned its first desalination plant to sustain socio-economic growth and development. The advancement coincided with a surprising discovery of two fresh groundwater caches in the Raudhatain and Umm Al-Aish depressions of northern Kuwait during a construction project (Parson's Corporation, 1961).

Subsequent studies reported two localized lenses of freshwater floating atop the upper saline aquifer in the Raudhatain and Umm Al-Aish areas of northern Kuwait, which are recharged from modern meteoric water despite adverse climatic conditions. After heavy rainfall, overland flow is channeled through wadis and concentrated in a topographic basin or playa, in which infiltration occurs through unsaturated surface sediments, and accumulates atop the saline aquifer to establish a stabilized lens configuration (Kwarteng et al., 2000; Viswanathan, 1997). Depression focused recharge (Lissey, 1971) and recharge originating within the wadi channel and annular periphery of the playa are the only supply of present-day freshwater resources in

Kuwait (UN-ESCWA, 2013). Sustainable yields and recharge rates ($1.0 \times 10^6 \text{ m}^3/\text{year}$) have been estimated for the isolated freshwater lenses, but were overestimated based on an alarming spike in total dissolved solids from 550 ppm to 1150 ppm between 1963 and 1969 (Kwarteng et al., 2000). Reduced extraction rates in step with above average rainfall improved conditions between 1970 and 1977. Estimates as high as $3.3 \times 10^6 \text{ m}^3/\text{yr}$ were proposed contingent upon above average rainfall amounts. Currently, the Raudhatain field produces $1.8 \times 10^6 \text{ m}^3/\text{yr}$ and the Umm Al-Aish field produces $0.8 \times 10^6 \text{ m}^3/\text{yr}$ (Al-Rashed and Sherif, 2000).

These amounts are a small fraction of Kuwait's water demand ($3.50 \times 10^8 \text{ m}^3/\text{year}$) (Hamoda, 2001). To prevent saltwater intrusion caused by over pumping, the State of Kuwait designated the lenses as a strategic water resource and restricted pumping to one water bottling company (Fadlelmawla et al., 2008). Water reports virtually ignore these freshwater resources by limiting the topic to a few sentences or omitting it completely. However, recent studies suggest the number of inland freshwater lenses in Kuwait and across similar arid regions of Western Asia are underestimated (Al-Sulaimi and Mukhopadhyay, 2000; Milewski et al., 2014). Moreover, shallow fresh groundwater ($< 100 \text{ m}$) in the form of perched lenses sustains oasis towns in Saudi Arabia, central UAE, Libya, and Egypt (Anderson, 2013; UN-ESCWA, 2013). Collectively, a growing list of locations suitable for inland lens occurrence implies freshwater inventories throughout the Arabian Peninsula are more abundant than currently known.

Furthermore, effects of climate extremes (droughts and floods) on precipitation, erosion, and recharge suggest that recharge type, and therefore location, may vary with climate regime (Meixner et al., 2016). Analyses of relationships between drainage densities and recharge location provide additional opportunities to identify inland freshwater lens occurrence in unexpected sites (Rotz and Milewski, 2014).

Investigations into formation, recharge, and degradation are required to properly assess impacts of extreme weather and human-induced processes on the sustainability of inland freshwater lenses. Presently, understanding of lens geometry and sustainability are limited. Early studies focus on water quality and age of northern Kuwait's freshwater resources, but recharge quantities and sustainability remain elusive (Al-Ruwaih and Hadi, 2005; Al-Ruwaih et al., 1998; Himida, 1981). Moreover, little information on "terrestrial" or inland lenses exists in the literature. Physical and analytical models developed by Fetter (1972), Van Der Veer (1977), Vacher (1988), and Stuyfzand and Bruggeman (1994) to calculate oceanic island lens thickness, length, and development under varying conditions cannot accurately predict inland lens parameter relationship and geometry due to differing boundary conditions. This primarily includes the recharge length parameter, which is assumed to be static and is not affected by the other parameters in the analytical solution for island lenses.

The major goal of this thesis is to examine the effect of recharge dynamics (e.g., rate, volume) on the formation and degradation of northern Kuwait's inland freshwater lenses. In particular, the following objectives are listed below:

1. Investigate the difference between island and inland lenses by way of lens geometry (i.e. thickness, length)
2. Examine the effect of recharge rate on lens formation by way of lens geometry (i.e. thickness, length)
3. Analyze the effect of recharge rate on lens degradation by way of lens geometry (i.e. thickness, length)

To achieve these objectives, a scaled physical model was used to simulate climatic, hydrologic, and topographic conditions of the Raudhatain watershed located in Kuwait. Varying recharge volumes were applied to the physical model and resultant inland freshwater lenses were measured through time using digital software. In addition to qualitative observations, regression analyses were performed with Microsoft Excel and R Programming Language. Results provided a model to predict the required time to maximum lens thickness, as well as a required time to minimum lens thickness based on respective formation and degradation rates as a function of recharge volume. Findings have practical implications for sustainable water resources management, including the calculation of immediately available freshwater and degradation rates after a recharge event in space and time.

The following chapters will contain regional climate, physiography, geology, and hydrology information of Kuwait; with a focus on northern Kuwait where known inland lenses exist. A literature review of inland freshwater lenses including new proposed locations, as well as an oceanic island analytical solution and discussion of the respective physical models are provided. Detailed specifications of the physical model design, implementation, and testing approaches are also provided in the methodology chapter. In addition, a report and discussion of results from this study, as well as a conclusion and summary are provided including an outline of recommendations for continued research on the topic.

Recharge processes in water-starved environments are often elusive and defy ready understanding. This investigation provides a unique opportunity to better understand the hydrologic cycle, particularly the relationship between depression focused recharge and variable-density ground water flow. Results provide a characterization of inland lens geometry, as well as the effect of recharge rate on formation and degradation. In addition, the information presented

in this study provides a baseline to improve temporal and spatial estimates of freshwater volume directly beneath recharge zones in Kuwait and other regions with similar geologic and hydrologic conditions. This research is important because the demand for freshwater throughout the Arabian Peninsula already exceeds available supplies, which are threatened by human and climate induced physical and chemical alterations (Lezzaik and Milewski, 2015; Werner, 2013). Achieving sustainability in arid environments like the Arabian Peninsula requires the implementation of diverse approaches to resources development and preservation (Omar, 1982). Insight into the occurrence and sustainability of inland lenses encourages water resources exploration and development in regions previously thought to contain no prospective new resources, as well as information for water resource managers interested in water quality preservation and artificial aquifer recharge in the same regions. While inland lenses cannot solve the problem of future water demands alone, they do provide drinking and agricultural water to indigenous people in remote areas and already serve as strategic and emergency water resources for Kuwait.

CHAPTER 2

SITE DESCRIPTION

The State of Kuwait is bordered to the north by Iraq, to the south by Saudi Arabia, and to the east by the Arabian/Persian Gulf (Figure 1). The country covers an area of 18,000 km² and is located in Western Asia on the northern edge of the Arabian Peninsula (29° 30'N, 45° 45'E). This study focused primarily on the Raudhatain and Umm Al-Aish regions located in the northeastern section of Kuwait where known inland freshwater lenses are currently utilized (Figure 2). However, climatic, geologic and hydrologic conditions across the Arabian Peninsula are similar. Therefore, this study is not only applicable to Kuwait but also throughout the Arabian Peninsula and other dryland environments in the world where conditions are similar.

2.1 Climate

Kuwait is characterized as a subtropical desert with an arid climate (Kottek et al., 2006). Summers are hot and dry, winters are mild, and annual rainfall is low (Figure 3). The average annual temperature is 26° C with an average maximum of 33° C and a minimum annual average of 19° C. Summer months are between June and August when temperatures can reach above 44° C, although May and September are also very warm. Winter temperatures are between November and March and can drop to 7° C. The rainy season coincides with the winter months, but rainfall is highly variable in both space and time. Kuwait City receives an annual average rainfall of 107 mm, with the wettest weather in January, averaging 26 mm / month (Climatemps, 2016). A maximum value of 336 mm of rainfall was recorded in 1954 and a minimum of 26 mm

was recorded in 1967. Average annual evapotranspiration (ET) exceeds rainfall as much as 2200 mm/year (Al-Sulaimi et al., 1997). Winter months experience the lowest ET rate at 4.9 mm/day (Ergun, 1969). Within the past 25 years, a positive correlation ($r^2 = 0.16 - 0.23$) exists between the tropical El Niño–Southern Oscillation (ENSO) and average rainfall at the interannual scale (Marcella and Eltahir, 2008). While only 16% - 23% of rainfall variability is explained by the ENSO occurrence, a statistically significant negative correlation ($r = 0.6 - 1.0$) exists between rainfall in Eastern Europe and Kuwait. In contrast, a positive correlation ($r = 0.9 - 1.0$) between rainfall in the eastern Mediterranean from November - April is observed.

Since 1970, Kuwait has experienced more frequent and higher magnitude periods of prolonged dryness. As a result, Kuwait is increasingly subjected to sand and dust storms, aeolian erosion, and sand encroachment (Khalaf and Al-Ajmi, 1993) (Figure 4). Winds originate primarily from the northwest and blow throughout the year. High wind speeds (> 5.5 m/s) frequently generate sandstorms, which occur during spring and summer months when a thick cloud of sand can be seen moving in the same direction of the wind (Membery, 1983). This is important to note because aeolian erosion and deposition processes change landforms across the Arabian Peninsula, which promote the formation and sustainability in inland freshwater lenses.

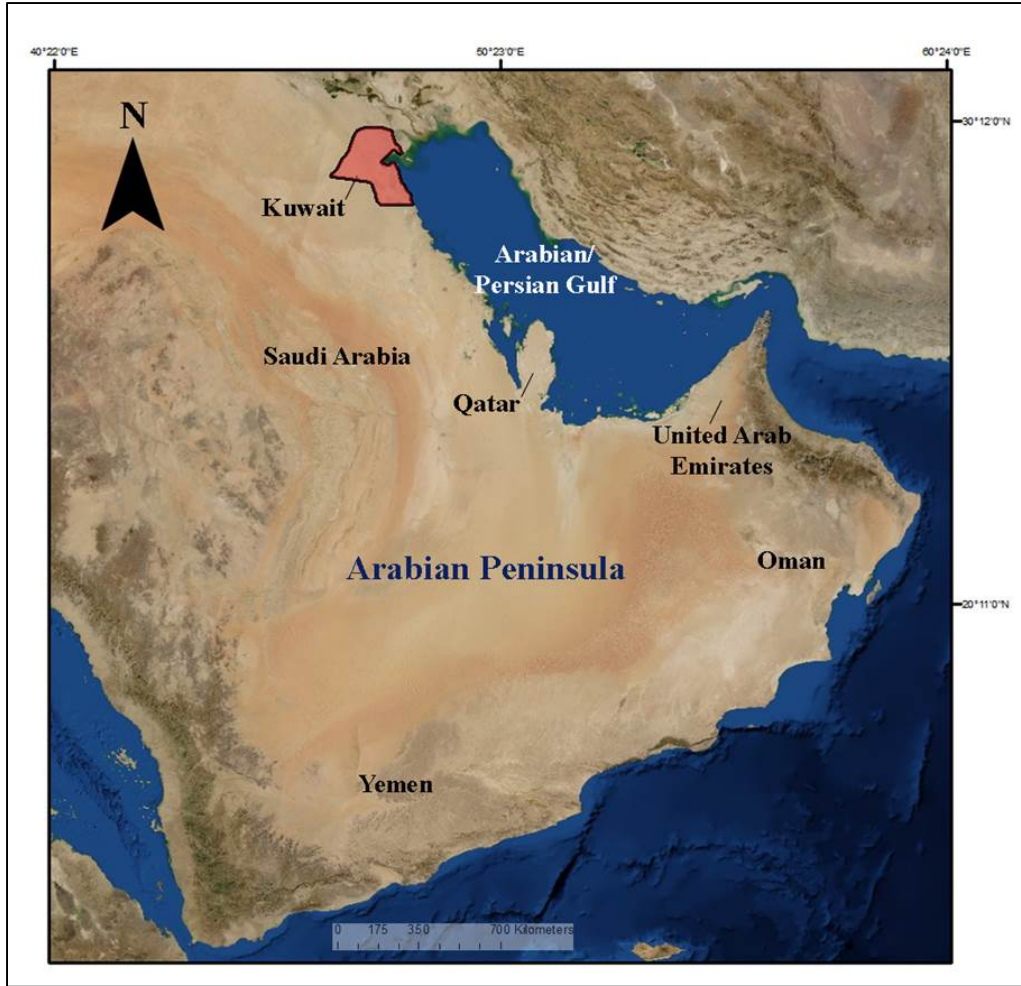


Figure 1. Map of Arabian Peninsula showing Kuwait highlighted in red along with other territories.

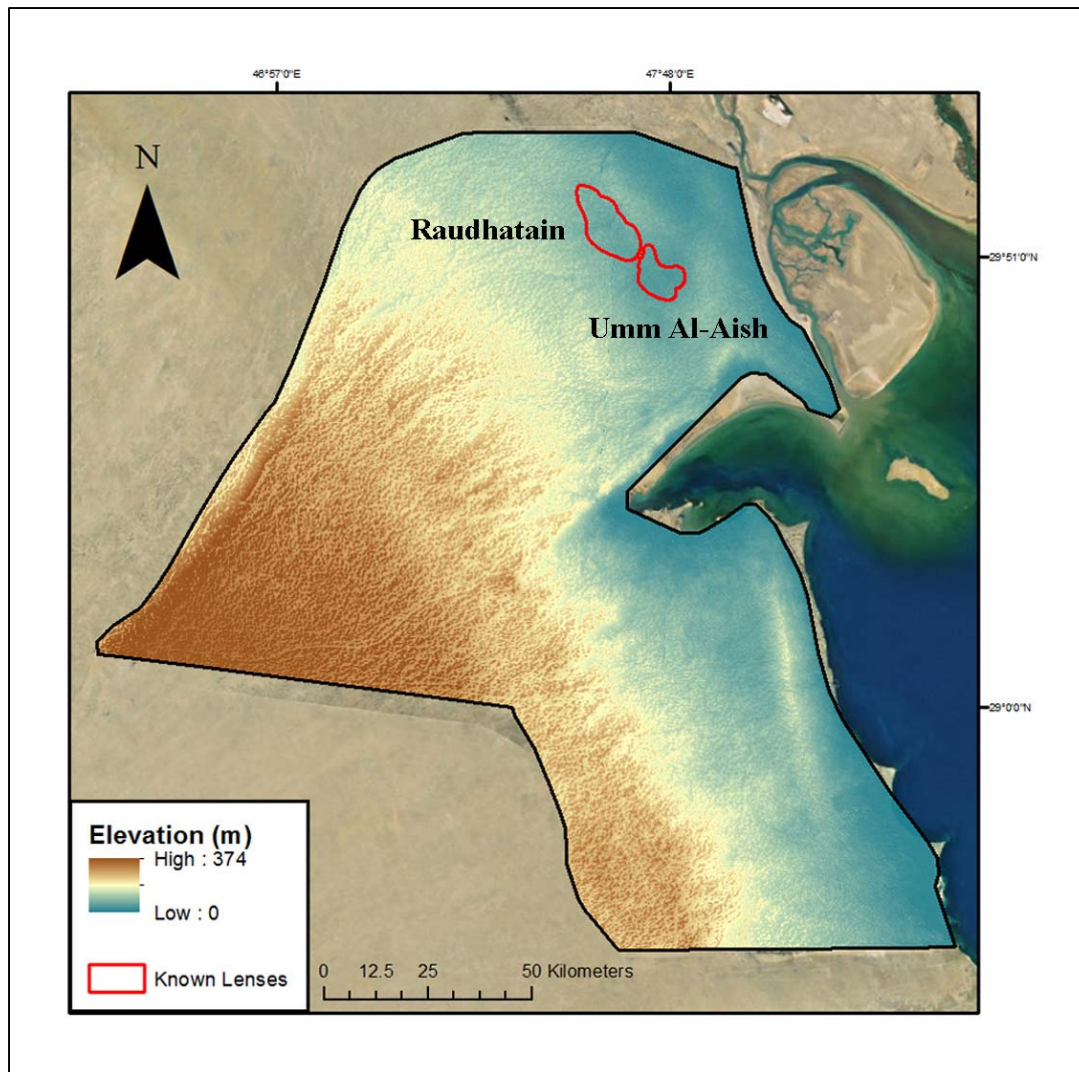


Figure 2. Elevation map of Kuwait and northern locations where known freshwater lenses occur.

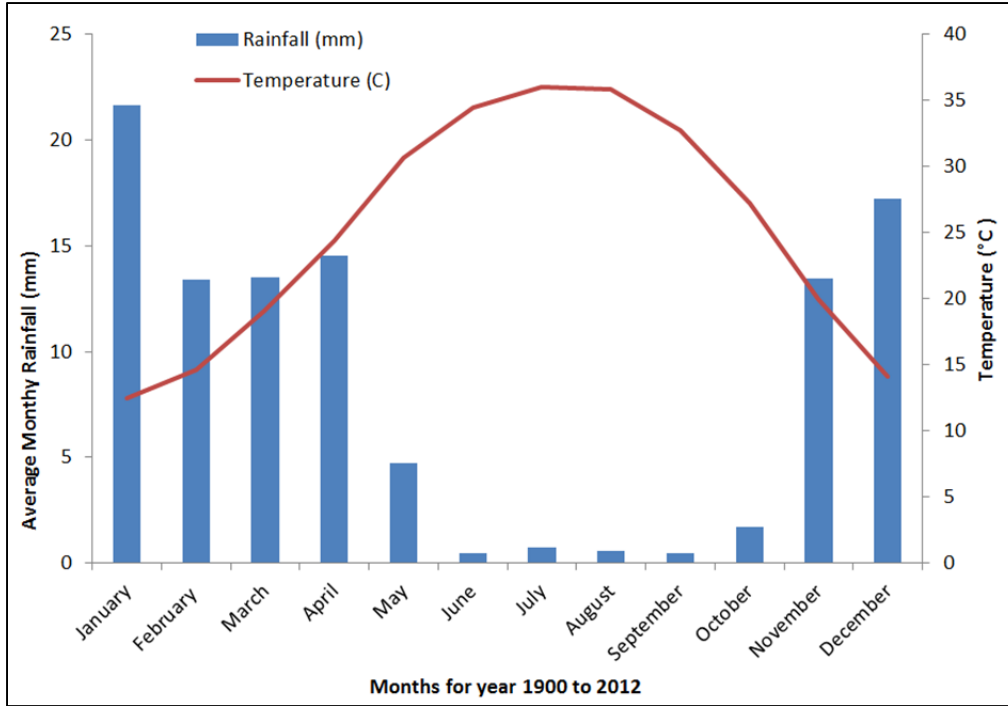


Figure 3. Temperature and precipitation values in Kuwait (University of East Anglia, 2016).

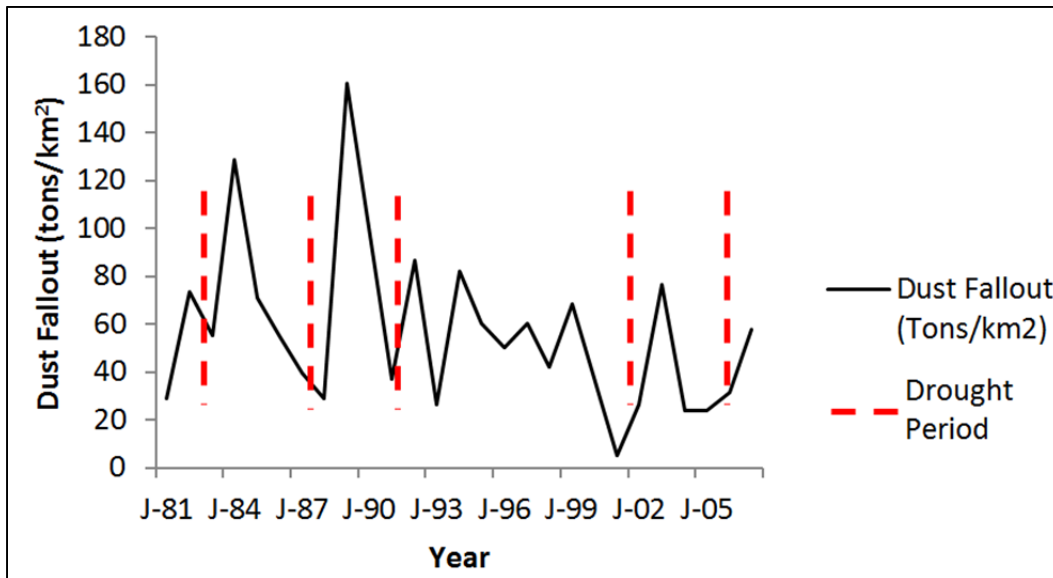


Figure 4. Comparison of dust fallout data and periods of prolonged drought characterized by Rotz and Milewski (2014) in northern Kuwait.

2.2 Physiography

The landforms in modern Kuwait are largely responsible for determining the locations of freshwater recharge and the occurrence of inland lenses. While Kuwait and the Arabian Platform are relatively flat (0.002), landforms are quite diverse (Figure 5). Undulating low hills, dunes, escarpments, and depressions result from wide climatic variations and increasing aridity from the Pleistocene epoch to present time, including aeolian processes, which contribute to the erosional and depositional features. These landforms combined with specific geologic and hydrologic conditions are necessary for inland freshwater lens formation and sustainability.

Elevations in Kuwait range from 300 m above sea level in the southwest to sea level along areas that border the gulf (Figure 6). One exception is the Jal Al-Zor Escarpment, which borders Kuwait Bay and rises more than 127 m above sea level. This surface feature bounds the southern region of the Raudhatain and Umm Al-Aish depressions. Wadis are another common feature and are found to incise the surface to as much as 48 m. A well-developed drainage network of wadis and gullies, which formed during ancient times when rainfall was abundant, cut across the country in a SW-NE direction. Resultant ridges, running parallel to the wadis, as well as alluvial fans are also commonly recognized (Al-Sarawi, 1995). Thin fan deposits (2.0 – 2.5 m) are located at the bottom of ridges and escarpments and contain valuable gravel deposits. Hills and low cuesta are scattered throughout the west but transition to a flat, deflated region in the central and northern regions of Kuwait. Shallow basins and playas occur on these flatter areas. Playas and dunes occur in the northeast depressions and are covered by water during the rainy season. Deeply incised channels, referred to as wadis, carry runoff to depressions and fracture depression walls en route, which promote mass wasting and colluvium deposition.

Unlike the dendritic drainage patterns of the wadis in the west, wadis in the northern regions form a centripetal pattern. These wadis drain into Raudhatain (790 km²) and Umm-Al-Aish (490 km²) watersheds (Bergstrom and Aten, 1965; Kwarteng et al., 2000). For example, twelve major wadis drain into the Raudhatain depression from all directions. In the subsurface, runoff slowly drains internally towards the Arabian/Persian Gulf (Alsharhan et al., 2001b). Figure 7 shows four areas in central and northern Kuwait where saturated conditions promote overland flow into local wadis, which transport runoff to topographic low areas and provide the necessary freshwater for depression focused recharge to occur. In northern Kuwait, the only two viable inland freshwater lenses occur beneath the Raudhatain and Umm Al-Aish depressions.

The Raudhatain depression is 80 km² and slopes from 3 m/km to the west and 4 m/km to the east of the lowest point which is 35 m above sea level. The interior depression of the Raudhatain is shallow and extends approximately 4.5 km wide from the east to west and 16 km long from north to south. The interior part of the Umm Al-Aish depression is approximately 20 km² with a slope between 4 m/km to the west and 6 m/km to the east. Several playas are located within the depression. Both Raudhatain and Umm Al-Aish bowl-like configurations dip in the direction of the regional northeastern slope (Al-Sulaimi and Mukhopadhyay, 2000) as a result of the regional gradient and geosyncline.



Figure 5. Landform examples that promote inland lens development across the Arabian Peninsula including a parabolic sand dune (left), deeply incised gully (middle) and the Jal Az-Zor Escarpment (right).

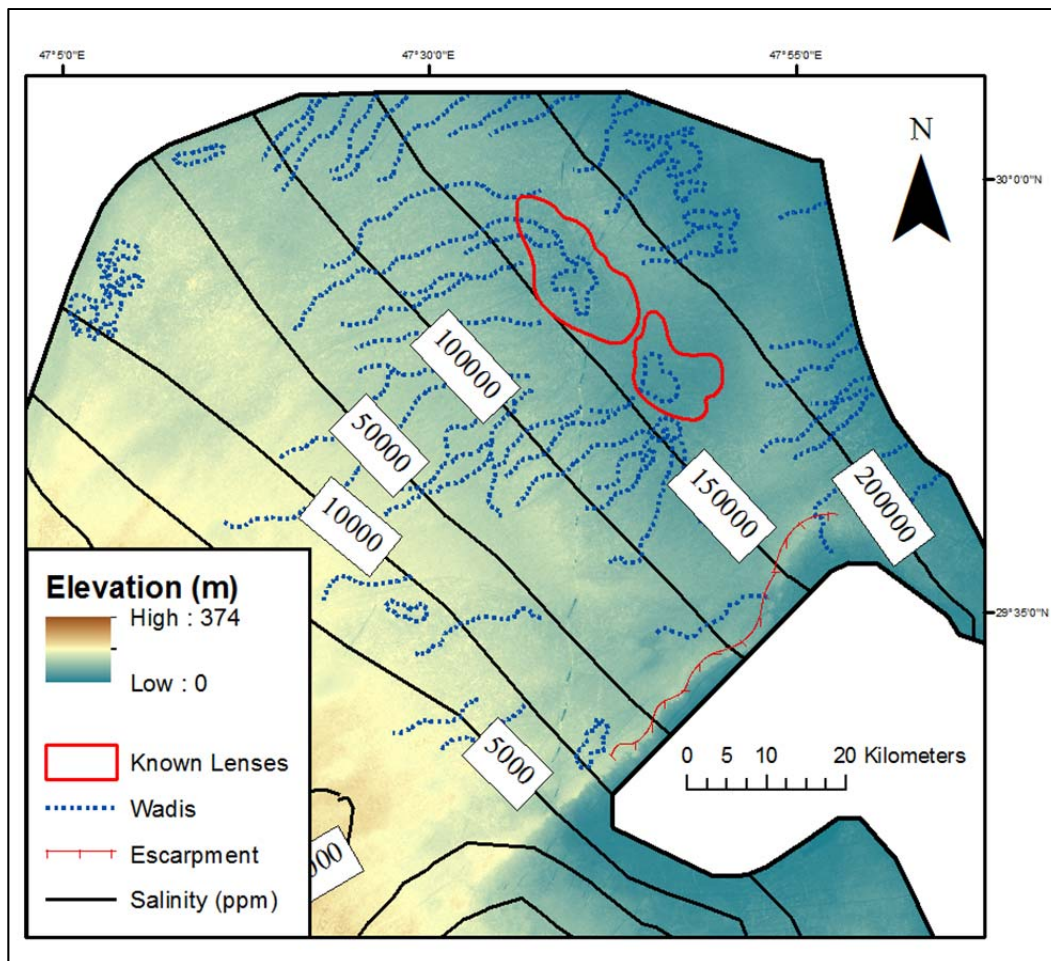


Figure 6. Areas of high elevation (yellow) transition to areas of low elevation (blue), while salinity levels (Abusada, 1988) increase in the direction of wadi flow. Centripetal drainage patterns of prominent wadi flow are shown terminating into the Raudhatain (top) and Umm Al-Aish (bottom) depressions where inland lenses occur.

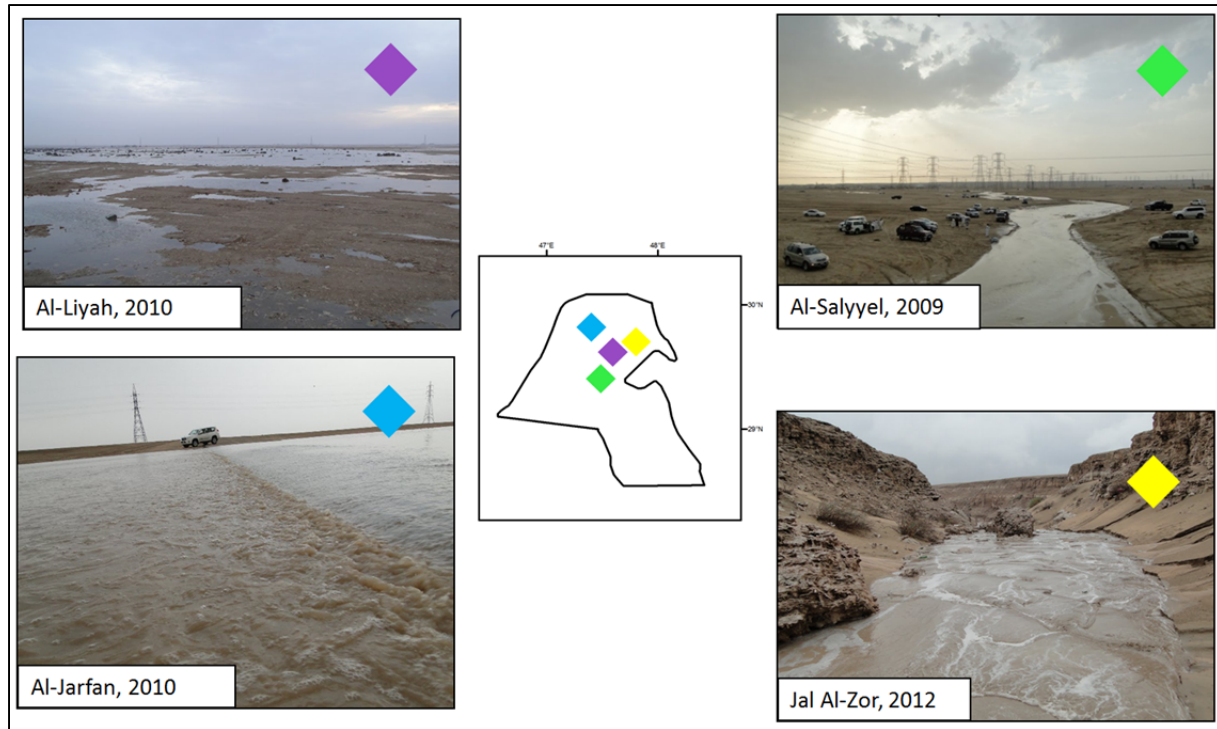


Figure 7. Four areas in central and northern Kuwait show saturated conditions where overland runoff is channeled to topographic depressions by local wadis.

2.3 Geology and Aquifers

Kuwait is located on the northeastern edge of the Arabian foreland on the Arabian Shelf, which was underwater during the accretion of the Arabian Shield for several marine transgressions throughout the Paleozoic and Cenozoic Eras (Alsharhan et al., 2001a). Increasing subsidence occurs outward from the Arabian Shield towards Kuwait, where a regional geosyncline is indicated by a thickening of sedimentary beds (Milton, 1968). These dynamics coupled with a humid paleoclimate during the Pleistocene period produced thick interbedded, gently dipping deposits of marine and fluvial sediments, which allow infiltration and storage of groundwater in more than thirty aquifer systems (Figure 8).

The uppermost, quaternary layer includes windblown sand, clay, playa silts, and wadi alluvium. These highly permeable unconsolidated sediments play a major role in freshwater lens formation and sustainability. Gypsum occurs throughout the layer, below surficial sediments at a depth of 10 – 20 cm and thins in the drainage areas around the playas. Caliche deposits are common and visible along gully walls (Al-Sarawi, 1995). The layer is sometimes white or pale yellow in color, laterally extensive, but limited vertically to 2 – 4 m below the surface. The caliche consists of pebbly, subangular to subrounded fragments of calcium carbonate embedded in a calcite matrix. The layer is explained by episodic deposition of sand and aeolian dust, which is considered the major source of ions for calcrete formation in Kuwait, during the Oligocene and Lower Miocene period (Al-Sulaimi, 1988). Wetter periods caused the downward percolation of CaCO_3 rich soil and contributed to the calcrete formation. The layer is fractured and weathered away in wadi channels and depressions (Al-Sarawi, 1995).

The Pleistocene Dibdibba Formation, the uppermost layer of the Kuwait Group, underlies recent sediments and is a principal aquifer for the region. Deposits include coarse gravel and sand, as well as conglomeratic sandstone, siltstone and shale. The Miocene Lower Fars Formation, also located within the Kuwait Group, contains conglomeratic sandstone, variegated shale, limestone, anhydrite and gypsum. Thickness extends more than 100 m beneath the Dibdibba formation but outcrops at the Jal Az-Zor Escarpment in the northeastern coast of Kuwait Bay, where the Um-Rimam depression is nestled in the northern edge of the escarpment (Figure 9). The Ghar Formation also outcrops at the base of the escarpment, but extends to depths as much as 300 m and contains oil. Subsurface rocks include Eocene limestone, which extends to depths as much as 1000 m with brackish water. Cretaceous limestone and shale range in thickness between 2000 and 3000 m and overlay early and pre-Cretaceous formations. The presence of highly water soluble evaporites promotes the brackish to saline groundwater conditions within the post cretaceous units up a depth of 100 m, where localized inland freshwater lenses float atop the saline aquifer.

Three sub-aquifers beneath in the Raudhatain and Umm Al-Aish depression hold potable groundwater (< 1000 ppm TDS). Production wells yield groundwater at depths of approximately 30 m below the surface from poorly sorted calcareous conglomeratic sandstone beds, which are separated by thin siltstone and shale beds. Localized freshwater continues to be found in upper layers of the Kuwait Group, but is progressively replaced by brackish and saline water within the lower groups and Dammam Formation. In the appropriately named Kuwait Group Aquifer, the water table ranges from 17 m to 50 m below the surface, depending on elevation, in the uppermost part of the saturated sandstone beds of the Dibdibba Formation. The maximum saturated thickness of water containing less than 1000 ppm of TDS is 33 m and water containing

less than 2000 ppm of TDS is between 10-20 m (Omar, 1982). The piezometric surface slopes northward and eastward in the direction of the regional gradient. Groundwater in the depressions is very fresh (200 - 1000 ppm TDS), but transitions to brackish (> 7000 ppm TDS) at depth and outside the depression.

Geologic conditions which promote groundwater salinity and include overlying, highly permeable, unconsolidated sediments are ideal for inland lens occurrence. While the regional geology described in this study focused on northern Kuwait, these geologic conditions are similar across the Arabian Peninsula, specifically the Arabian Platform.

Age	Group	Formation	Thickness	Graphic Log	Description	Groundwater Conditions
Recent			< 30 m		Beach sands and limestones; wind blown sand; playa silts and clays; wadi alluvium	Unsaturated zone with local fresh and brackish water depending on drainage and topographic position
Pleistocene	Kuwait	Dibdibba	112 m		Coarse gravel and sand; conglomerate sandstone; siltstone shale	High permeability of shallow aquifer; water locally fresh beneath depressions, brackish at depth
Miocene		Lower Fars	110 m		Fine to conglomeratic calcareous sandstone; variagted shales; fossiliferous limestone; gypsum	Low permeability; localized fresh water beneath depressions; brackish water
		Ghar	288 m		Quartose sandstone and conglomerate; some shale	Deep groundwater; brackish
Eocene	Hasa	Dammam	192 - 223 m		Discontinuous chert caps; chalk and siliceous limestone; dolostone	Moderate permeability; moderately brackish water
		Rus	80 - 128 m		Anhydrite; limestone; marl	Brackish water
		Radhuma	191 - 448 m		Marly limestone; dolomite	Brackish water

Figure 8. Regional geology of northern Kuwait after Bergstrom and Aten (1965).

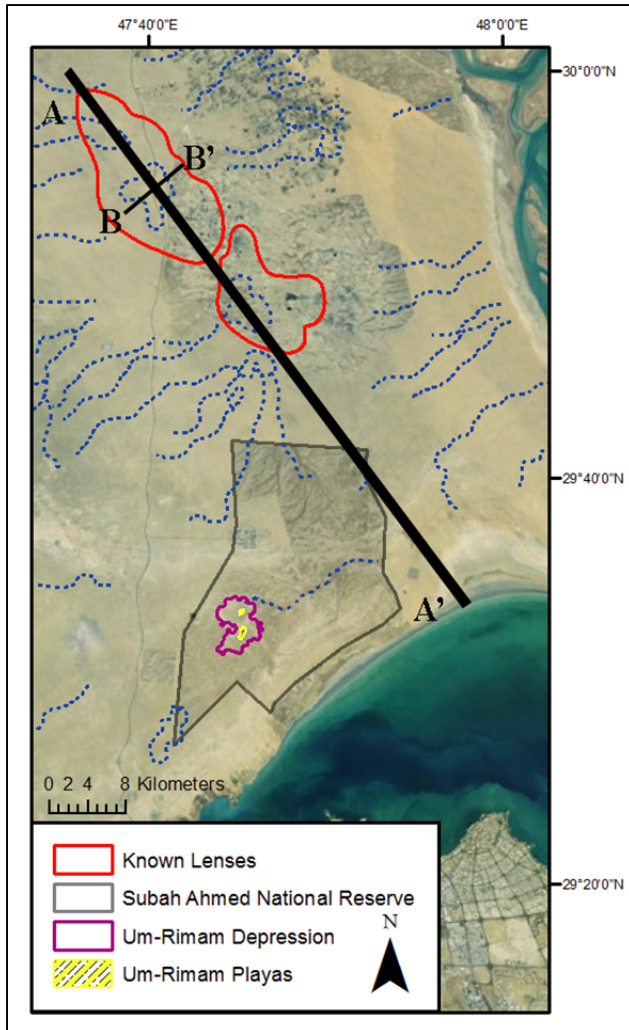


Figure 9. Map of northern Kuwait showing cross-section lines. The map also shows the Subah National Reserve, which contains the Um-Rimam depression. Playas are highlighted in yellow.

2.4 Hydrogeology and Water Quality

The hydrostratigraphic units of the region include the Kuwait Group, Dammam, Rus, and Umm Er-Radhuma Formations in descending order. Along with the Kuwait Group, the Dammam formation is a principal aquifer for the region. Together, the two aquifers create a hydrological system that provides relatively continuous flow from southwestern to northeastern Arabian Peninsula (Figure 10). Groundwater is primarily recharged in the northeastern part of Saudi Arabia through the Hasa Group, home of the Dammam Formation. Salinity increases steadily in the direction of the regional gradient (NNE to SW) and becomes brackish by the time it reaches Kuwait. In the Kuwait Group, CaSO_4 and NaCl dominated waters are the most abundant brackish water types, whereas $\text{Ca}(\text{HCO}_3)_2$ and $\text{Na}(\text{HCO}_3)_2$ are water types for freshwater fields (Al-Ruwaih et al., 1998). Overwithdrawal and saltwater mixing is a concern. Salinity is low but increases with depth due to the presence of localized freshwater lenses in northern Kuwait. Water quality problems in freshwater lenses began early when pumping induced rapid deterioration due to an overestimation in yields and were immediately reduced in 1988 from 9000 m^3/d to 180 m^3/d to preserve water quality. However, after twenty years, salinities have not returned to initial levels (Kwarteng et al., 2000).

Hydrologic parameters have been measured at six zones on the surface and subsurface of northern Kuwait (Tables 1-3). Bergstrom and Aten (1965) estimated groundwater movement in the Kuwait Group of about 0.03 - 0.67 m/d from south to north based on permeability, porosity, and gradient. Transmissivities of the Kuwait Group aquifer were estimated at 295-3456 m^2/d . Transmissivities decreased eastward towards the Arabian/Persian Gulf (Al-Ruwaih et al., 1998). Measured infiltration rates of surface sediments in Kuwait were reported to average 28.8 cm/h but ranged as high as 67 cm/h, whereas average wadi deposits and depressions were measured as

much at 10.4 cm/h (Al-Ruwaih and Hadi, 2005). Hydraulic conductivities of surface sediments ranged from 3.4×10^{-2} to 2.25×10^{-2} m/s between 0 – 210 cm and decreased to as much as 8.2×10^{-5} m/s in the upper aquifer of the Kuwait Group (Al-Ruwaih and Hadi, 2005; Al-Sarawi, 1995). Further, a sharp decrease was recorded at the gatch layer at a depth of 210 cm from 1.47×10^{-2} m/s to 2.25×10^{-2} . This sharp decrease suggests that the gatch layer acts as a moisture barrier, which encourages the lateral movement of freshwater down gradient.

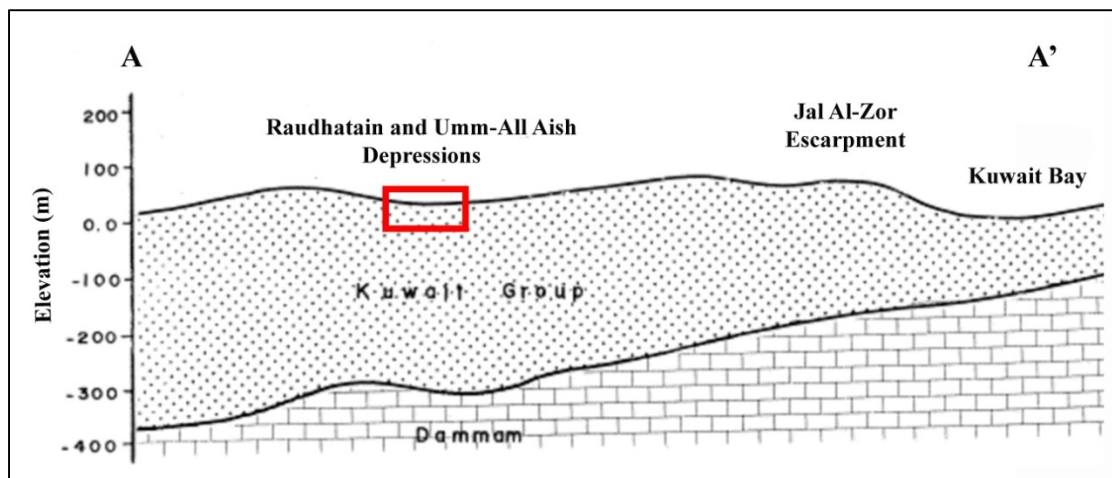


Figure 10. Surface topography and relative aquifer thicknesses of northern Kuwait from north (A) to south (A'). Highlighted red area shows the approximate location of Raudhatain and Umm Al-Aish fresh water lenses after (Al-Sulaimi and Mukhopadhyay, 2000).

Table 1. Surface sediment measurements of saturated hydraulic conductivity from an oil field in southern Kuwait (Al-Sarawi, 1995).

Depth from Surface (cm)	K sat m/s
0-30	3.4×10^{-2}
30-90	1.4×10^{-2}
90-155	1.3×10^{-2}
155-210	1.16×10^{-2}
210-250 (gatch)	1.8×10^{-3}
250 -300	1.3×10^{-3}
Average	1.26×10^{-3}

Table 2. Infiltration rates summary of northern Kuwait surface sediments (Sayed et al., 1992).

Surface Sediment Type	Max Infiltration (cm/h)	Max Infiltration (cm/h)	Average Infiltration (cm/h)
Upper Dibdibba (sand and gravel)	67	6	28.8
Sheet wash deposits (fine gravel and sand)	25.5	10	17.4
Lower Dibdibba (cemented calcareous sandstone)	24.6	10.5	17.4
Undifferentiated Fars and Ghar Formations (friable sand)	34	16	26.6
Wadi deposits and depressions (silty sand)	16	4	10.4

Table 3. Kuwait City aquifer parameters (Sayed et al., 1992).

Main Unit	Subunits	Type	Hydraulic Parameters
Upper Kuwait Group Aquifer (localized lenses at depths of 0-100m)	Upper	Water Table Aquifer	T (m ² /s) 1.22 x 10 ⁻³ K _h (m/s) 8.2 x 10 ⁻⁵ K _v (m/s) 8.2 x 10 ⁻⁷ S _y 0.1
	Middle	Aquitard	K'/b'(s ⁻¹) 5.78 x 10 ⁻¹⁰
	Lower	Semiconfined Aquifer	T (m ² /s) 1.96 x 10 ⁻³ S 6.00 x 10 ⁻⁴

T = transmissivity (m²/s)

S = storage coefficient

S_y = specific yield

K_h = horizontal hydraulic conductivity of the aquifer (m/s)

K_v = vertical hydraulic conductivity of the aquifer (m/s)

K' = vertical hydraulic conductivity of the aquitard (s⁻¹)

b' = aquitard thickness (m)

CHAPTER 3

LITERATURE REVIEW

Cumulative geological, hydrogeological, and geochemical research has improved understanding of freshwater resources in Kuwait. In 1961, the Parson's Corporation of Los Angeles, California discovered freshwater (~600 ppm TDS) in the Raudhatain area during a construction project (Parson's Corporation, 1961). Subsequent studies have characterized many geologic and hydrogeologic aspects of the area (Bergstrom and Aten, 1965; Kwarteng et al., 2000; Milewski et al., 2014; Omar et al., 1981; Parson's Corporation, 1961, 1964; Senay, 1977; Viswanathan, 1997). In addition, physiographic and climatic analyses contribute to understanding the relationship between atmosphere, land surface, and inland lens occurrence and potential recharge (Al-Awadhi et al., 2014; Al-Sulaimi et al., 1997; Al-Sulaimi and Mukhopadhyay, 2000; Khalaf and Al-Ajmi, 1993; Rotz and Milewski, 2014). The culmination of this research has provided a wealth of information to characterize required conditions for inland freshwater lenses occurrence in hot, arid desert environments.

3.1 Climate Variability and Recharge in Kuwait

Drought is a serious concern in arid environments and directly impacts water resources. In addition to extreme conditions (i.e. low rainfall, high evapotranspiration), climate variability and anthropogenic activities affect aeolian processes, sand encroachment, dune patterns, and vegetation (Al-Dabi et al., 1997; Khalaf and Al-Ajmi, 1993; Kwarteng and Al-Ajmi, 1996). Kuwait has experienced a number of prolonged dry periods since 1970 where rainfall was below

the annual average. Misak et al. (2013) and Rotz and Milewski (2014) identified and correlated periods of prolonged dryness to shifting sands (Figure 11). Results showed that stream density decreased during dry regimes. In addition, remote sensing images showed drainage channels belonging to the Umm Al-Aish depression in the Subah Ahmed National Reserve filled with dust during times of high dust fallout (Figure 12). Khalaf and Al-Ajmi (1993) reported high rates of sand encroachment during summer months caused by human activities and desertification. Links between the aforementioned studies and their effect on recharge are relatively new but suggest a connection between drought and recharge dynamics (e.g. location, type), specifically in arid environments (Meixner et al., 2016; Scanlon et al., 2005; Taylor et al., 2013). Landscape variation, including recent aeolian deposition and erosion, are indicators of recharge mechanism variation, and therefore potential indicators of buried recharge zones.

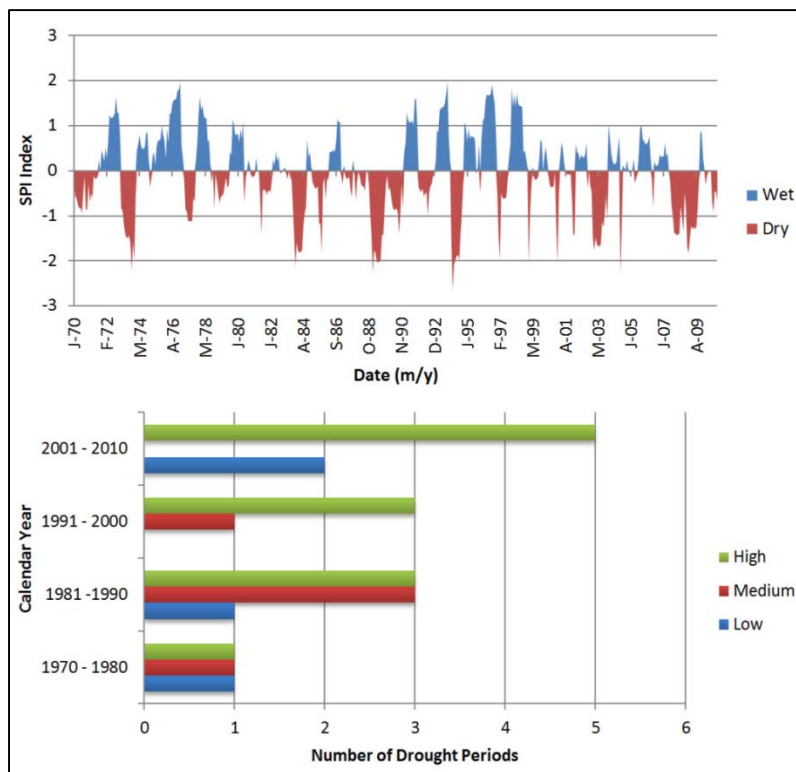


Figure 11. SPI Index and drought characterization indicates increasing periods of dryness (Rotz and Milewski, 2014).

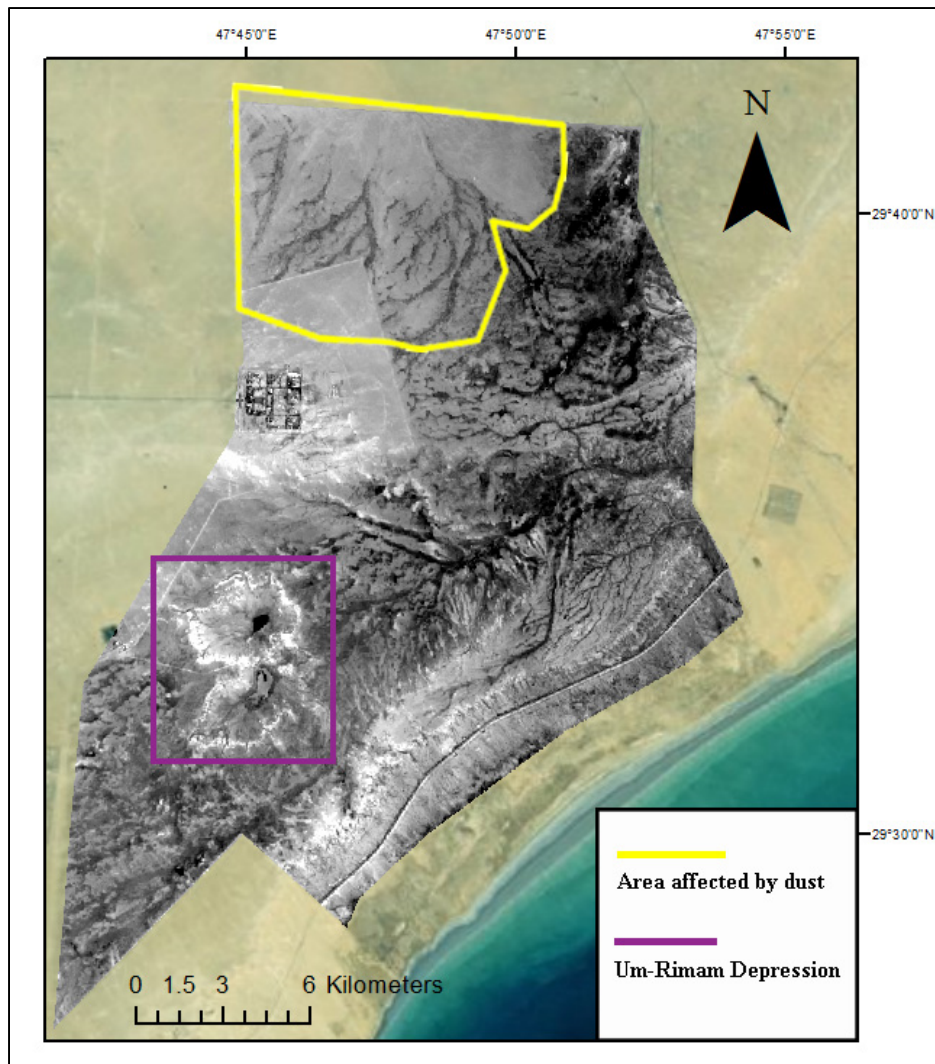


Figure 12. Dust fills wadis draining to Umm Al-Aish Depression after major drought-induced dust storm in Subah Ahmed National Reserve. Um-Rimam Depression contains surface water visible from satellite image suggesting a recharge zone and potential inland lens (Rotz and Milewski, 2014).

3.2 Lens Recharge

Parson's Corporation (1964) designated three localities within the central playas of the depressions as zones of infiltration and subsequent recharge, despite conflicting measurements of highly variable albeit low infiltration rates in the surface sediment. Bergstrom and Aten (1965) also arrived at the same conclusion during one of the earliest investigations into the freshwater resources of Raudhatain and Umm Al-Aish areas. The study analyzed water quality and age and reported that the highest water quality and youngest water reside directly beneath the playas at the lowest elevations of the depression. However, comparisons between estimated recharge ($180 \text{ m}^3/\text{d}/\text{km}^2$) and available water for rainfall ($350 \text{ m}^3/\text{d}/\text{km}^2$) not only implied unusually low evapotranspirative loss, but also substantial runoff to the depression, which had never been observed due to the rarity of intense storms. Pan evaporation tests measured evapotranspiration rates at $27 \text{ cm}/\text{mo}$ and soil moisture deficiencies in the playas did not correspond to the idea that recharge occurred directly above the playa surface. Grealish et al. (1998) compared vertical infiltration rates ($2 \text{ cm}/\text{h}$) in the centers of the depression to adjacent wadi channels ($60 \text{ cm}/\text{h}$) and asserted that recharge originates from wadi channels and at the periphery of the depression where the wadi terminates.

While this suggestion agreed with infiltration measurements, it still conflicted with groundwater quality measurements directly beneath the depression center, which was suspected to be more deteriorated if water infiltrated into the subsurface farther from the depression center. Fadlilmawla et al. (2008) noted groundwater in the Raudhatain depression was undersaturated with respect to halite, which agreed with the absence of this mineral in the top soil by XRD analysis. The study also compared Carbon-14 activities in groundwater to atmospheric concentrations and identified three locations where recharge is likely to occur. Viswanathan

(1997) developed the concept of the “gatch” layer extending from 10 cm - 2 m from the surface, which was briefly mentioned in Bergstrom and Aten (1965), as the mechanism delivering freshwater to the depression center (Figure 13). He proposed that freshwater migrated laterally along a relatively impermeable layer to the depression center, where the hard caliche-like layer of calcareous rock is eroded, and water is free to flow vertically towards the freshwater lens. This process is referred to as depression focused recharge and is a requisite condition for inland freshwater lens occurrence (Lissey, 1971).

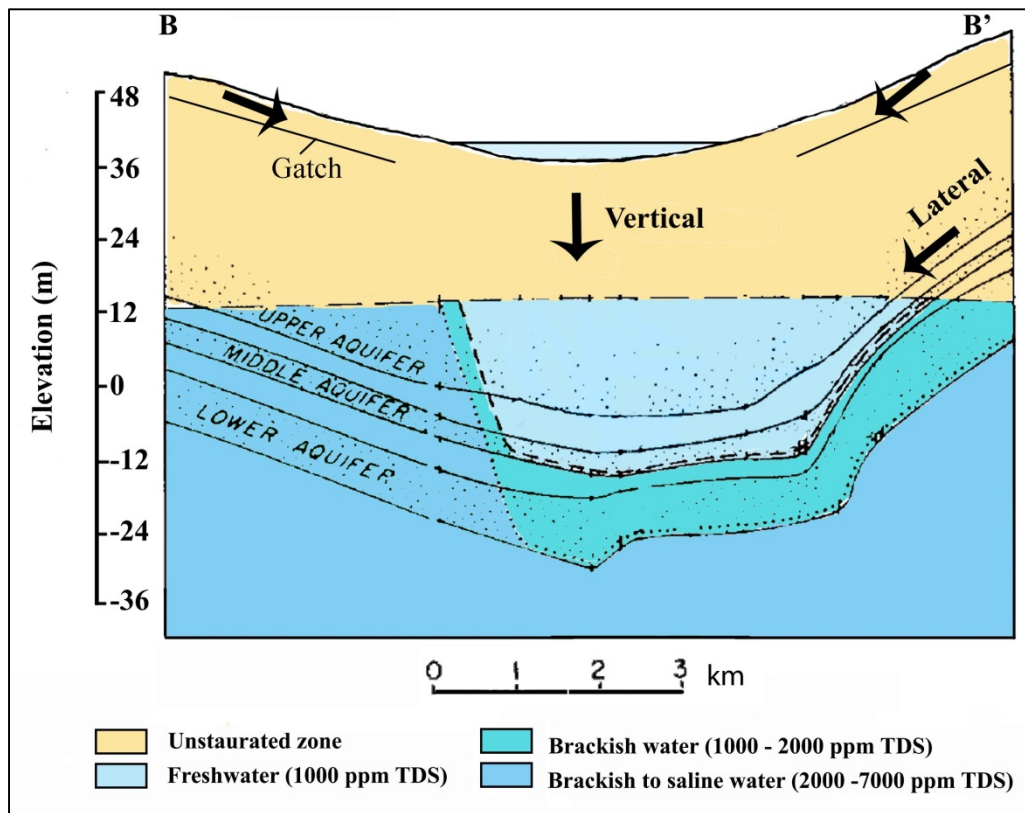


Figure 13. Cross-section of Raudhatain Depression from west (B) to east (B') showing water table, permeable and semipermeable layers of the Kuwait Group aquifer, as well as vertical and lateral recharge to the freshwater lens after Bergstrom and Aten (1965).

3.3 Geomorphic Analyses and Lens Locations

In northern Kuwait, physiography has been investigated to explain how fresh groundwater continues to accumulate in spite of extreme aridity (Al-Sulaimi et al., 1997; Al-Sulaimi and Mukhopadhyay, 2000; Al-Sulaimi and El-Rabaa, 1994; Kwarteng et al., 2000; Milewski et al., 2014). Al-Sulaimi and El-Rabaa (1994) created a morphostructural map of Kuwait which was later examined with Kuwait's drainage system to determine morphometric parameter relationships between wadi systems, playas and recharge locations (Al-Sulaimi et al., 1997). As a result, eleven prospective areas for near-surface groundwater in Kuwait were proposed (Al-Sulaimi and Mukhopadhyay, 2000). In addition, large-scale observational tools such as earth orbiting satellite sensors, geographic information systems, and computer modeling have enabled temporal and spatial integration of geoscience data to promote sustainable water resource development (Becker, 2006). These methods are a powerful tool in improving understanding of the Earth's surface, as well as subsurface groundwater conditions in inaccessible areas. A study by Kwarteng et al. (2000) integrated a paleo-drainage map with a Digital Elevation Model satellite image to show the proximity of drainage channels and elevation contours in northern Kuwait.

Milewski et al. (2014) expanded this approach. The study integrated digital elevation data, precipitation (Tropical Rainfall Measuring Mission), lithology, wind, soil moisture (Advanced Microwave Scanning Radiometer for EOS), surface temperature (Advanced Very High Resolution Radiometer) and vegetation (Normalized Difference Vegetation Index), along with the Soil Water Assessment Tool model to identify favorable locations for freshwater lens development. The study identified more than twenty locations likely for inland lens occurrence and a total of 142 possible locations in Kuwait and throughout the Arabian Peninsula (Figure

12). Results include thirteen highly prioritized locations for in-situ verification. One example is the Um-Rimam depression nestled in the northern edge of the Jal Az-Zor Escarpment. Freshwater is seen from satellite images indicating ponding and subsequent recharge (Figure 10 and Figure 14). The efficiency and scale to which novel techniques like these can be used are useful for water resource exploration en masse. These results imply that renewable freshwater resources in Kuwait and across the Arabian Peninsula are underestimated and underpin the importance of characterizing inland freshwater lenses.

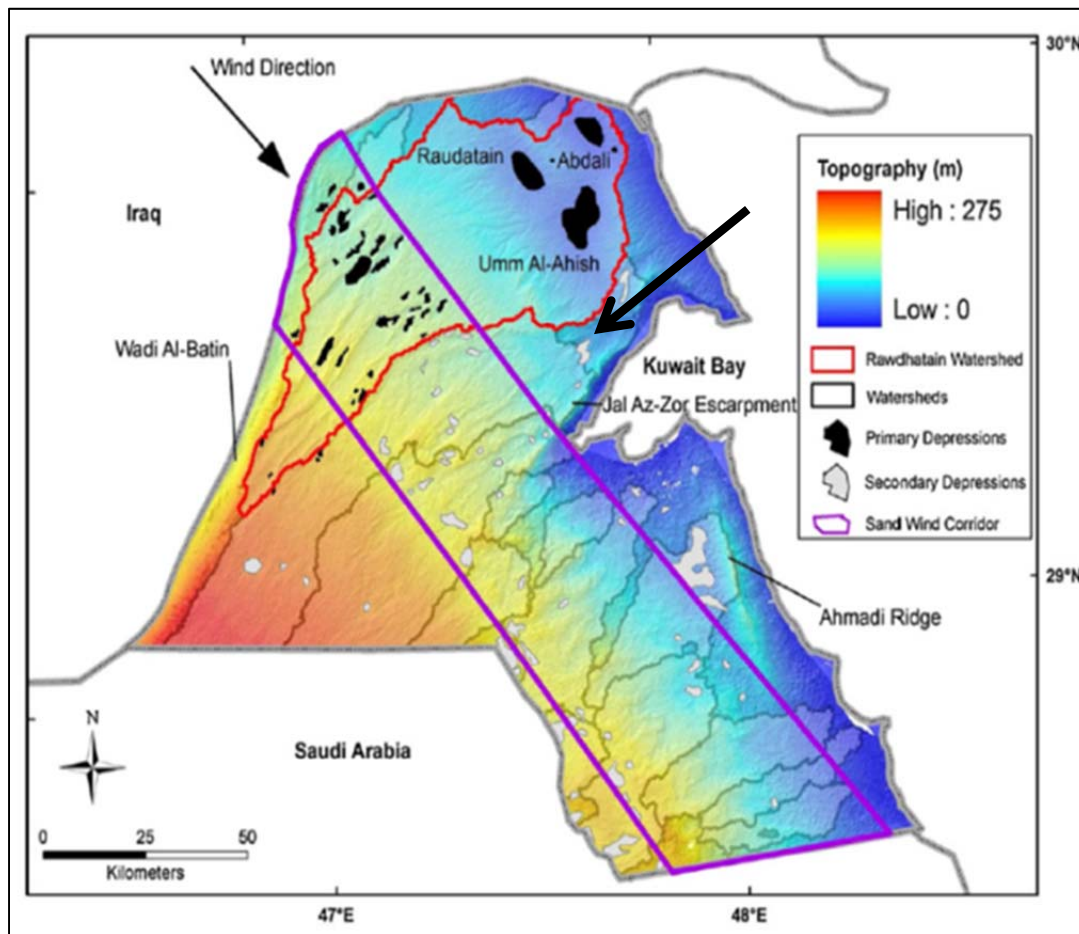


Figure 14. Proposed recharge zones and subsequent freshwater lens locations throughout Kuwait including Um-Rimam depression indicated by the arrow after Milewski et al. (2014).

3.4 Oceanic Island and Inland Lenses

Fresh groundwater that floats atop saline water is most common in oceanic and coastal hydrology (Figure 15). In these cases, an island is completely surrounded by seawater. Rainfall infiltrates downward towards the saltwater table and accumulates atop the denser seawater to form a lens. The island freshwater lens is relatively stable beneath the surface due to the surrounding saltwater (Werner, 2013). Early analyses began surrounding fundamental variable-density studies by Baydon-Ghyben (1898) and Herzberg (1901), who characterized the freshwater/saltwater interface in a coastal aquifer. Research into the geometry and volume of island freshwater lenses is the topic of several investigations and presented analytical solutions for isotropic and anisotropic conditions (Fetter, 1972; Vacher, 1988; Van Der Veer, 1977).

Some authors have dealt with a freshwater wedge in a coastal aquifer (Glover, 1959; Henry, 1964). Terrestrial freshwater lens investigations are rare but do exist (Eeman et al., 2012; Houben et al., 2014; Werner and Laattoe, 2016). Houben et al. (2014) utilized geophysical techniques to create a water budget and measure lens geometry of an inland lens 900 km from the coast in Chaco Paraguay. Results showed typical behavior of a freshwater lens. However, the author noted that thickness deviated from a Ghyben-Herzberg lens and suggested a confining layer was responsible.

Eeman et al. (2011) examined controlling factors for shallow rainwater lenses in deltaic areas in the Netherlands and identified a gradual mixing zone between rainwater and saline seepage. Werner and Laattoe (2016) presented an analytical solution to define the depth of the saline freshwater interface for a freshwater lens that flowed into a river atop a saline aquifer. Like the aforementioned studies, Carol et al. (2010) determined that the groundwater flow of a

local freshwater lens off the coast of Argentina is strongly dependent on recharge conditions, by which travel times were calculated utilizing an analytical solution by Chesnaux and Allen (2008).

Boundary conditions for both oceanic and terrestrial lens studies differ dramatically from the inland lenses of northern Kuwait. For oceanic lenses, no-flow boundaries are defined at the edges of the islands at the shoreline due to the surrounding saltwater. In the terrestrial lens study by Werner and Laattoe (2016), the shoreline boundary condition was replaced with a freshwater river, and the underlying saline aquifer flowed towards the river while the overlying freshwater lens remained stable. All approaches include the Dupuit assumption of horizontal flow and Darcy's Law, which are combined to form the Dupuit-Ghyben-Herzberg (DGH) analysis (Bear, 1972).

Like the analytical and numerical models found in the literature, physical models of freshwater lenses are primarily limited to coastal and island lenses. However, much can be learned about salt and freshwater interaction from physical models (Dose et al., 2014; Pennink, 1915; Stoeckl and Houben, 2012; Zhao et al., 2009). These models successfully show formation and degradation of island lenses, flow paths, and steady state lens thickness as a function of recharge. In these cases, an acrylic tank was constructed to simulate island lens formation. Stoeckl and Houben (2012) observed results and tested performance against an analytical solution from Vacher (1988), and a numerical solution to show lens dynamics with varying hydraulic conductivity conditions. Dose et al. (2014) followed a similar approach where travel times and age stratification were analyzed.

The literature reviewed for this study is relevant to understanding the necessary conditions for inland lens development beyond the oceanic island and coastal lenses. While it has been shown that an awareness of inland freshwater lenses exists within the scientific community, distinguishing research into modeling of inland freshwater lenses is sparse. The lack of information regarding the physical characteristics and behavior of the inland lenses of Kuwait provides an opportunity to explore this unique and valuable resource, while also contributing to the scientific discourse of inland freshwater lens dynamics.

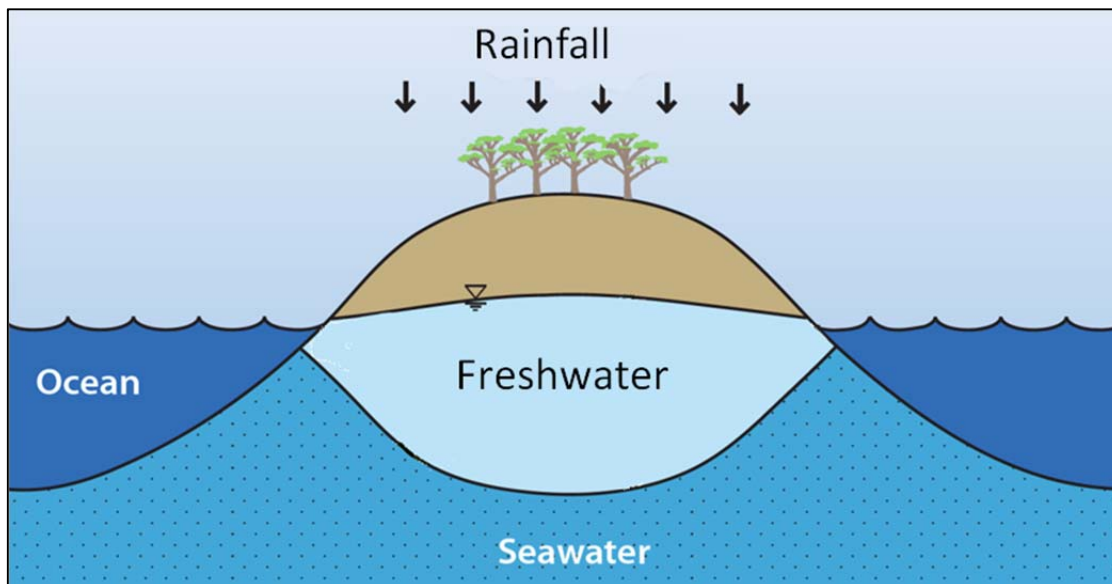


Figure 15. Typical oceanic island lens schematic after Werner (2013).

CHAPTER 4

METHODS

4.1 Objectives

Despite the abundance of geochemical and hydrogeological research on freshwater lenses in northern Kuwait, physical models of freshwater lenses are limited to island oceanic lenses. As a result, many questions regarding inland lens geometry, formation, and degradation are unanswered, not only in Kuwait but also worldwide. A large amount of time and energy must be devoted to answering questions regarding the available volume of freshwater through space and time. This study focused on examining the differences between inland and island lenses, but also investigating the effect of recharge on inland lens formation and degradation. In particular, the following objectives are listed below:

1. Investigate the difference between island and inland lenses by way of lens geometry (i.e. thickness, length)
2. Examine the effect of recharge rate on lens formation by way of lens geometry (i.e. thickness, length)
3. Analyze the effect of recharge rate on lens degradation by way of lens geometry (i.e. thickness, length)

Physical Model

Previous studies have utilized physical models to investigate oceanic island freshwater lenses (Dose et al., 2014; Pennink, 1915; Stoeckl and Houben, 2012; Zhao et al., 2009). At the beginning of this study, a physical model was designed and built to simulate a cross-section of a topographic depression overlaying a saline aquifer using scaled values of the depressions in

Kuwait (Figure 16). The approach was based on a physical model utilized for an infinite strip island by Stoeckl and Houben (2012). An acrylic tank (2.0 m x 1.0 m x 0.10 m) was conceived to hold sand and water, as well as to allow water to drain out of the bottom and side of the tank (Figure 17). The top of the tank remained opened but was covered with an acrylic lid. A 13 mm slit extended along the top of the lid and served as a guide to hold the precipitation tubes in place. Twelve basal and three right-sided drainage holes spaced every 150 mm, accommodated 13 mm threaded fittings with 10 mm barbed ends. Polyurethane plastic tubing controlled by plastic valves drained water from the drainage holes into catchment buckets. A 38 mm diameter by 1 m tall PVC pipe was installed on the inside left side of the tank to add saline water back into the tank. The PVC was perforated 40.75 cm along the right side of the bottom half of the pipe to encourage saltwater flow from the left to the right side of the tank. Low flow peristaltic pumps were utilized to add both freshwater and saltwater into the tank. Power was supplied to the pumps with a Philmore Multi-Voltage Regulated DC power supply. Recharge was pumped through 3 mm polyurethane plastic tubing adhered to the tank lid over the depression center. To visualize recharge and freshwater accumulation, fluorescent tracer dye was added at 15 mL/gallon. The effects of the tracer dye on the freshwater were assumed to be negligible. Instant Ocean® marine salt was utilized to create 35,700 ppm TDS saltwater. The salinity of both fresh and saline water was determined using a salinity refractometer. The results with their respective conversions are shown in Table 4.

Table 4. Salinity measurements and conversion of fresh and saline water.

	Salinity (ppt)	Relative Specific Gravity (sg)	Specific Conductance (mS/cm)	Density (kg/m³)	Parts-Per-Million TDS
Freshwater	<1	~1.001	~1.013	~1000	~649
Saltwater	37	1.028	55.75	1028	35700

Medium to fine sand, determined by a standard test method particle size analysis with a sieve kit, filled the tank to replicate the unconsolidated surface sediment. Grain distribution results characterized sand as 5.2% gravel, 93.8% sand, and 1% fines (Figure 18). Total porosity was calculated using the sum of solid and pore volumes and estimated at 22%. Sand was moderately well to well sorted. The saturated hydraulic conductivity was measured using a steady state permeameter at a value of 1.5×10^{-3} m/s. Other assumptions include homogenous soil, symmetrical depression, two-dimensional model, and a relatively flat hydrologic gradient with regional groundwater flow. Figure 19 shows the model when filled with sand prior to running a simulation.

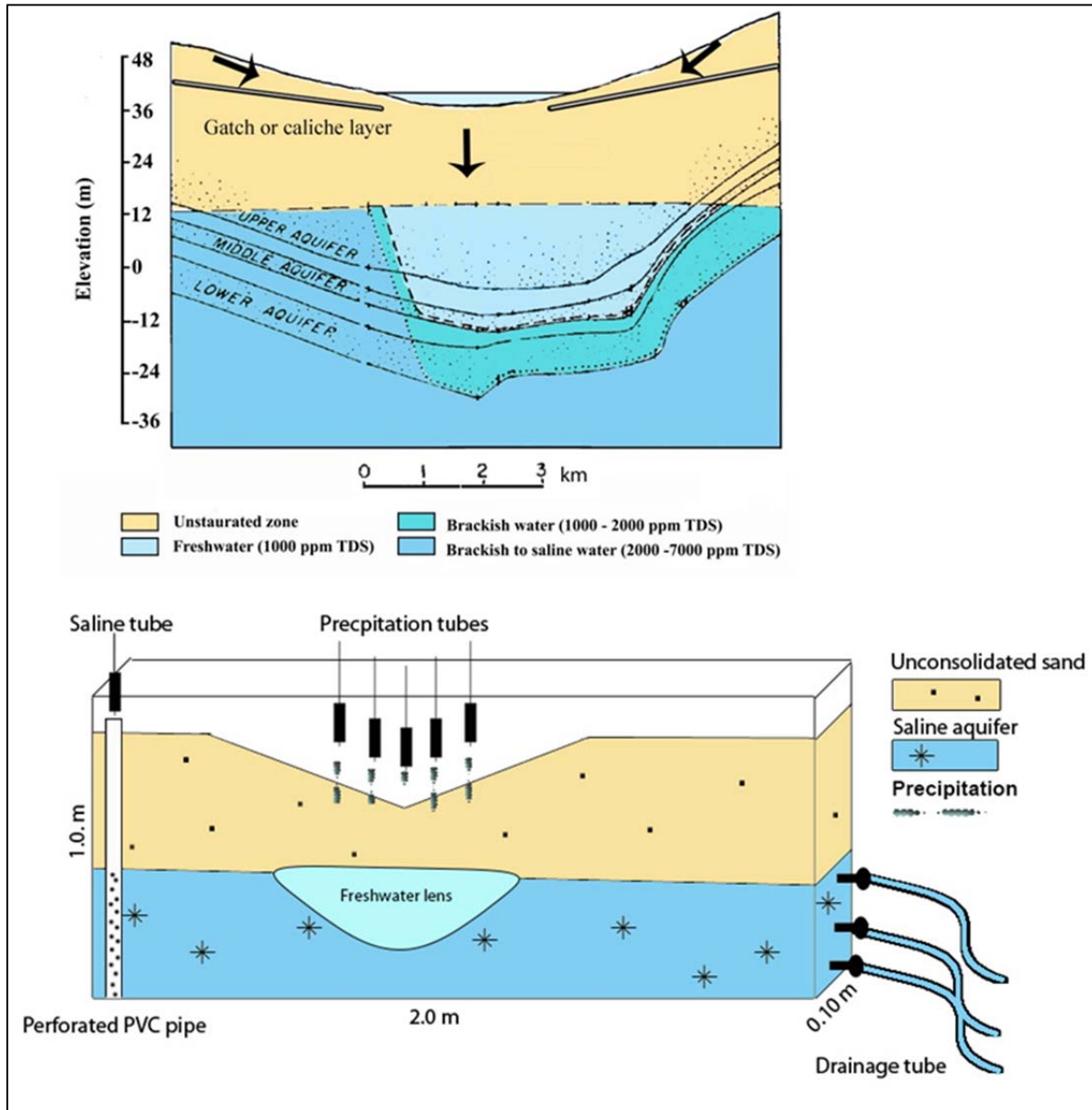


Figure 16. Cross-section of Raudhatain depression (top) after Bergstrom and Aten (1965) motivates concept for the physical model to simulate an inland freshwater lens.



Figure 17. The physical model, power supplies, valves, pumps, and sand counter clockwise from left to right.

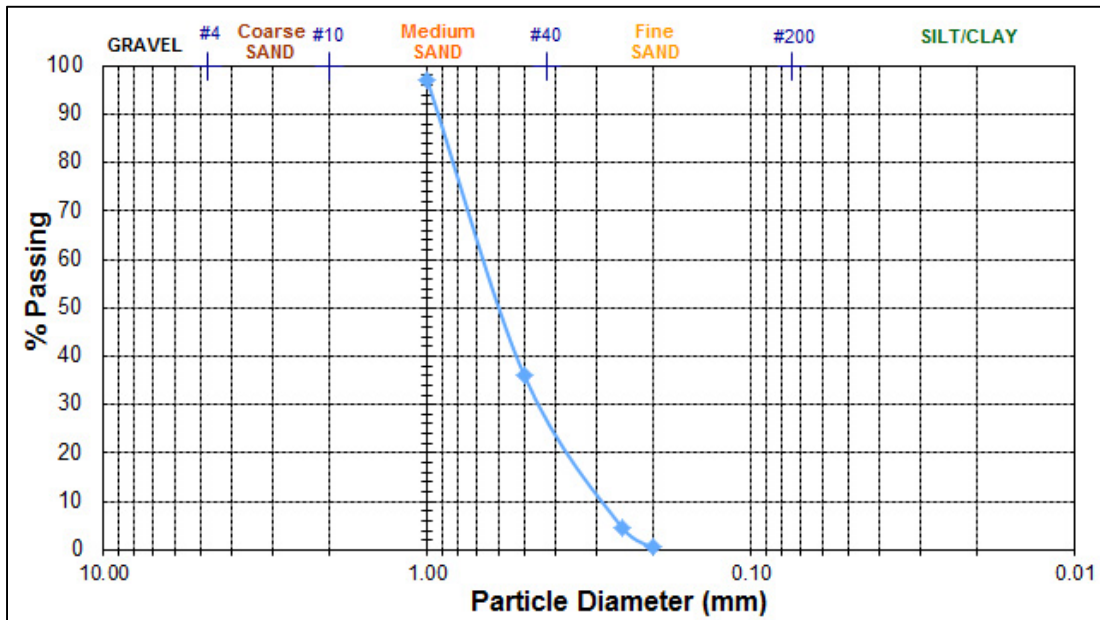


Figure 18. Grain size analysis using standard test method for particle size analysis of soils. Grain distribution curve results are 5.2% gravel, 93.8% sand, and 1% fines.

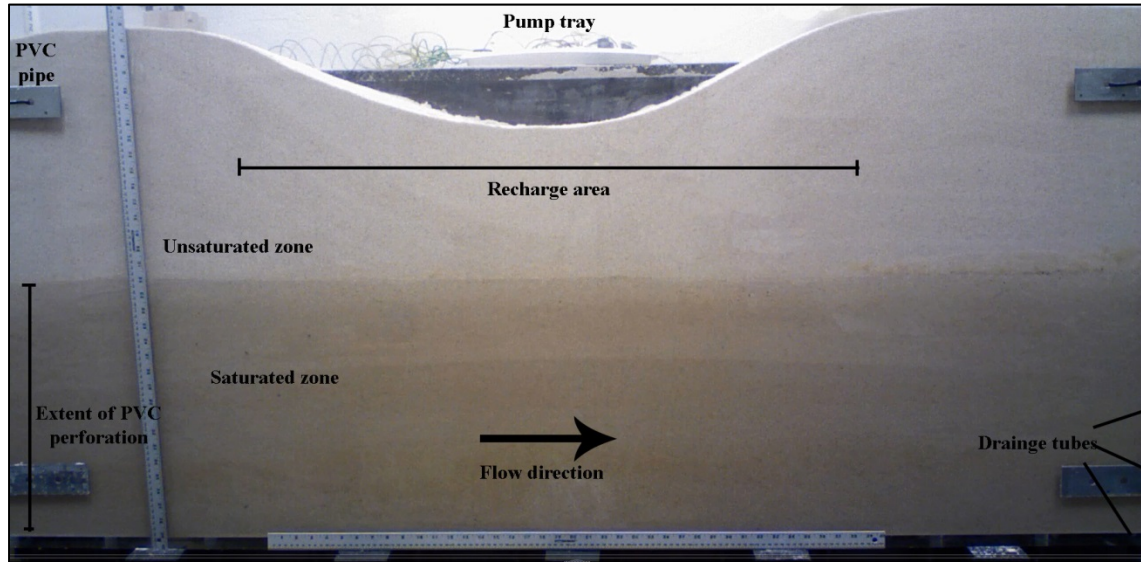


Figure 19. Physical model setup before simulation.

4.3 Simulations

In each simulation, the tank was systematically filled and packed with sand to a height of 43 cm from the bottom of the tank. Saltwater was slowly poured into the left side of the tank until the sand appeared saturated. A minimum time of 24 hours was given for the air to move out of the saturated zone. Dry sand was then slowly poured and packed on top of the saturated zone on the left and right sides of the tank to form a depression in the center. Depression length was constrained to approximately 1 m for all simulations. The number of drippers mounted above the depression varied between eight and five for the first three simulations but were reduced to three drippers for the remaining six simulations. Recharge areas also varied to determine the best model configuration in earlier simulations and were kept between 0.045 and 0.050 m after simulation #4. Recharge was applied for a period of 60 min. Recharge rates varied between 50ml/min to 175 mL/min. In all, nine simulations were administered; four with no flow of the underlying saline aquifer and five with an average saline aquifer flow rate of 13 mL/min. Simulations were digitally photographed every thirty seconds for the duration of the simulations with a Brinno TLC200 time-lapse camera at 720 dpi resolution. Two meter-long measuring sticks were placed on the outside of the tank and utilized to calibrate digital measuring software. Freshwater lens length and thickness were measured visually using WebPlotDigitizer software. A video of each simulation was compiled with the time lapse images (Appendix A). The location or height of the freshwater table was approximated due to a capillary fringe that formed in the unsaturated zone. Hence, a total thickness was measured in all simulations which combined the estimated height of the freshwater table and the depth to the fresh saltwater interface ($z+h$). Lens length (L) was the other parameter measured (Figure 20).

4.4 Differences between Island and Inland Lenses

Nine simulations were simulated to observe the difference between island and inland lenses. The saturated saltwater zone did not flow out and no new saltwater was introduced during the first four simulations. A maximum lens thickness (D_o) was visually determined, at which time thickness measurements were taken at positions along an x-axis, as well as a length measurement. In previous studies of island freshwater lenses, a Dupuit-Ghyben-Herzberg (DGH) analytical model by Vacher (1988) combined the Ghyben-Herzberg principle with horizontal flow to predict the relationship between the depth to interface below sea level and the elevation of the freshwater table above sea level assuming uniform recharge and hydraulic conductivity. Measurements of observed maximum thickness (D_o) were compared with the maximum thickness derived by the analytical solution (D_a). The variables used are as follows:

h_f	freshwater table elevation above sea level (m)
h_s	saltwater table elevation at sea level (m)
K	hydraulic conductivity (m/s)
R	recharge rate (m/s)
ρ_f	freshwater density (kg/m^3)
ρ_s	saltwater density (kg/m^3)
x	horizontal coordinate (m)
L	width of island cross-section (m)
α	density ratio by Ghyben-Herzberg (m)
z	depth to interface (m)

Points along the water table were chosen in increments of 0.04 m and the water table elevation was calculated after Vacher (1988) using:

$$h^2 = \frac{R}{K(\alpha + 1)} * (Lx - x^2)$$

The depth to interface (z) for any point (x) along the water table was calculated using the Baydon-Ghyben (1898) principle:

$$z = \left(\frac{\rho_f}{\rho_s - \rho} \right) h_f \left[\text{where } \alpha = \frac{\rho_f}{\rho_s - \rho_f}, \text{ therefore } z = \alpha h_f \right]$$

The observed lenses simulated with the physical model were visually fitted to analytical lenses to show differences in length and thickness. In addition, statistical analysis was performed using R Programming Language and Microsoft Excel to show the relationship between length and thickness as a function of recharge.

4.5 Recharge Rate on Lens Formation and Degradation

The last five simulations (6-10) were used to investigate inland lens formation and degradation. Lens formation analysis included measuring the time required for a lens to fully develop, or time of maximum thickness (T_{max}). This was determined at the time when the rate of change equals zero before the lens begins to degrade. Lens degradation analysis included measuring lens thickness and length after T_{max} . To simulate flowing groundwater, new saltwater was introduced into the saturated zone, while previously added saltwater flowed out of the opposite side at a steady-state rate of 13 mL/min. A similar approach to analyzing the difference between island and inland lenses was also used for the part of the study. Video files were reviewed and the time of maximum thickness (T_{max}) was visually established, at which time length and thickness measurements were taken. Statistical analysis was performed to show the effect of recharge on maximum lens thickness.

The same five simulations were administered to measure the rate of change of lens thickness and the rate of change of lens length through time after the lens fully developed. Measurements occurred every 3600 seconds from the start of the simulation, but only measurements at and after the time of maximum thickness (T_{max}) were considered for this part of the analysis. All measurements terminated on or before 43200 seconds (12 hours) when the lens

migrated close enough to the tank wall to become distorted. Statistical analysis was performed to show the effect of recharge rate on degradation.

4.6 General Comments on the Physical Model

The physical model possesses specific limitations. Although the model is intended for a two-dimensional analysis, a width of 0.10 m must be noted. Therefore, some fluid is not observable during the experiment. In addition, sand was cleaned and dried between each simulation. Then the sand was added back into the tank. This resulted in variation of sand sorting for each simulation. Overall, this seemed to minimally affect the results; however, freshwater water did seep up through preferential flow paths (Figure 20). Lastly, the three peristaltic pumps utilized primarily had a minimum consolidated recharge output volume of 50 mL/min. Therefore, it was difficult to perform simulations with lower recharge amounts. The pump used to add water to the saline aquifer was a low flow pump enabling 13mL/min for aquifer flow; however, saltwater recharge was applied at a length of 40.75 cm on the left side but only flowed out of the bottom two tubes on the right side at a height of 25 cm.

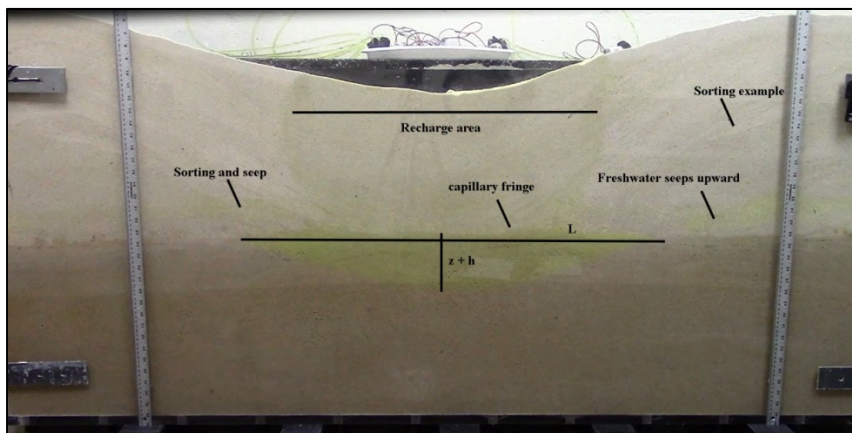


Figure 20. An example of simulation measurement parameters. L = length, z = depth to interface, and h = elevation of lens above water table. While some freshwater flowed through preferential pathways due to sorting, the lens was distinguishable.

CHAPTER 5

RESULTS AND DISCUSSION

The simulations successfully generated nine freshwater lenses over varying recharge rates and time-dependent conditions. Appendix A provides an example of time lapse photos for simulation 6. Recharge areas varied primarily in the earlier simulations. Table 5 provides simulation parameters including hydraulic conductivity (K), recharge area and length, recharge rate (R), Ghyben-Herzberg ratio (α) and saltwater flow rate (Q). The first four simulations were performed with no saltwater flow, whereas the remaining five experiments included a flow of 13 mL/min or 1×10^{-6} m/s. Vertical infiltration to the saltwater table and freshwater accumulation atop the saline head were observed after freshwater was applied to the center of the depression. Lens thickness and length increased with time until the lenses reached a maximum thickness, after which time length continued to increase and thickness decreased. Lenses extended laterally in the direction of the saltwater flow until it reached the tank wall and distorted.

Table 5. Parameter values for all simulations. K = saturated hydraulic conductivity, R = recharge, Q = saltwater flow. Recharge calculations based on recharge length.

Sim	K (m/s)	R Area (m ²)	R Length (m)	R (mm/hr)	R (m/s)	R Volume (ml/min)	α	Q (m ³ /s)
2	0.0015	0.05	0.5	126	1.39E-04	417	36	0
3	0.0015	0.104	1.04	106	5.61E-05	350	36	0
4	0.0015	0.06	0.6	28	2.56E-05	92	36	0
5	0.0015	0.042	0.42	17	2.20E-05	56	36	0
6	0.0015	0.045	0.45	15	1.85E-05	50	36	2.17E-07
7	0.0015	0.05	0.5	30	3.27E-05	98	36	2.33E-07
8	0.0015	0.045	0.45	53	6.48E-05	175	36	2.33E-07
9	0.0015	0.045	0.45	19	2.33E-05	63	36	2.33E-07
10	0.0015	0.05	0.5	18	2.00E-05	60	36	2.17E-07

5.1 Analytical and Observed Lens Comparison

Objective: Investigate the difference in lens geometry between inland and island lenses.

The simulated lens did not fit the analytical solution in all simulations, despite recharge rate. Lens thickness or depth to freshwater and saltwater interface was less than the analytical solution at all positions. Observed lens length was greater than the length of the analytical solution, which is constrained by a no-flow boundary condition in the analytical solution for the island lens (Figure 21).

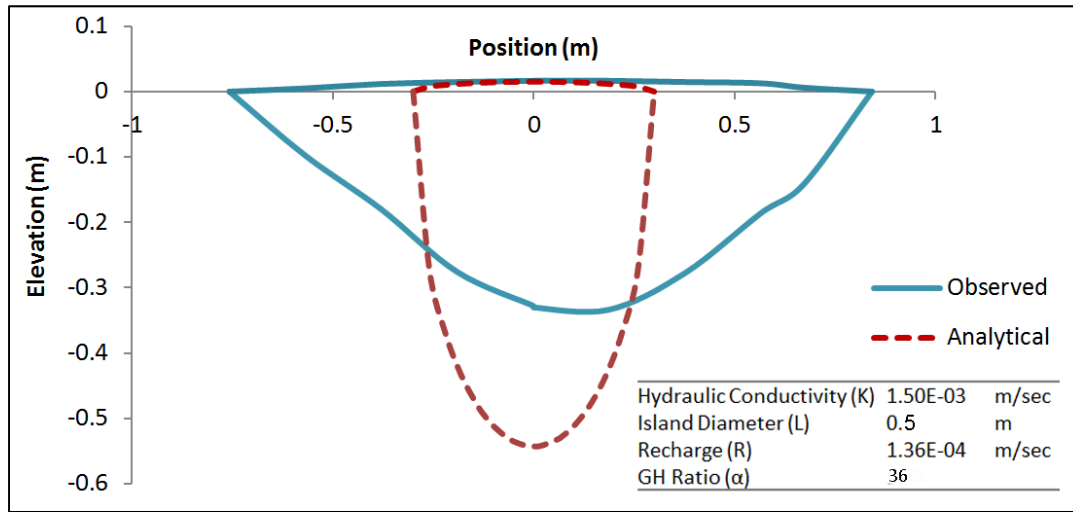


Figure 21. Simulation observed vs. Vacher (1988) analytical solutions. Right table shows actual parameter values.

Lens thickness ($z + h$) and lens length (L) were measured. As recharge rates increased, maximum lens thickness (D_o, D_a) and length (L_o, L_a) at time of maximum thickness increased for both the analytical and observed lenses (Table 6). The relationship between recharge rate and thickness can be seen for both observed and analytical lenses by the following log-log regression:

$$D_o = 701.61 * R^{0.855}$$

$$D_a = 62.741 * R^{0.5317}$$

As recharge rates increased, length at time of maximum thickness increased also increased for analytical and observed lenses by the following log-log regression:

$$L_a = 1.5451 * R^{0.1142}$$

$$L_o = 1.8428 * R^{0.5395}$$

Figures 22 and 23 compare thicknesses and lengths of observed and analytical lenses for all nine simulations, including simulations #3 and #4, which have higher recharge areas (1.04 and 0.60 m) than the other seven simulations. Outlier data points for simulations #3 and #4 in Figures 22 and 23 show recharge areas do affect lens thickness and length measurements and were removed in Figures 24 and 25. Comparison of the y-intercepts of both regressions of simulations with similar recharge areas show lens thickness for the analytical solution was greater than the observed during simulations (Figure 24). Analytical solutions generated lenses that were, on average, 58% thicker than observed lenses and 59% shorter but varied with recharge rate.

These results emphasize the constraint of the analytical solution and difference between oceanic island lenses, which are bound by the length of the island while inland lenses flowed freely in these experiments (Figure 25). Further, these results correspond with the poor fit of the observed to analytical lens demonstrating that inland maximum lens thickness is characteristically less than island lenses, while inland lens length is longer at the time of maximum lens thickness. While both lens thickness and length are positively correlated to recharge for both freshwater lens types, observed lens length is more positively correlated to recharge than analytical lenses due to the differences in the boundary conditions of the two lens types.

Table 6. Parameter values for all nine simulations. R = recharge, z+h = thickness, L = length.

Sim	R Area (m²)	R (m/s)	z+h (m) (Analytical)	z+h (m) (Observed)	L (m) (Analytical)	L (m) (Observed)
2	0.050	1.39E-04	0.57	0.330	0.60	1.600
3	0.104	5.61E-05	0.60	0.190	1.04	1.670
4	0.060	2.56E-05	0.28	0.107	0.60	0.920
5	0.042	2.20E-05	0.19	0.070	0.42	0.467
6	0.045	1.85E-05	0.19	0.059	0.45	0.540
7	0.050	3.27E-05	0.27	0.108	0.50	0.748
8	0.045	6.48E-05	0.35	0.200	0.45	0.923
9	0.045	2.33E-05	0.21	0.078	0.45	0.587
10	0.050	2.22E-05	0.23	0.075	0.50	0.640

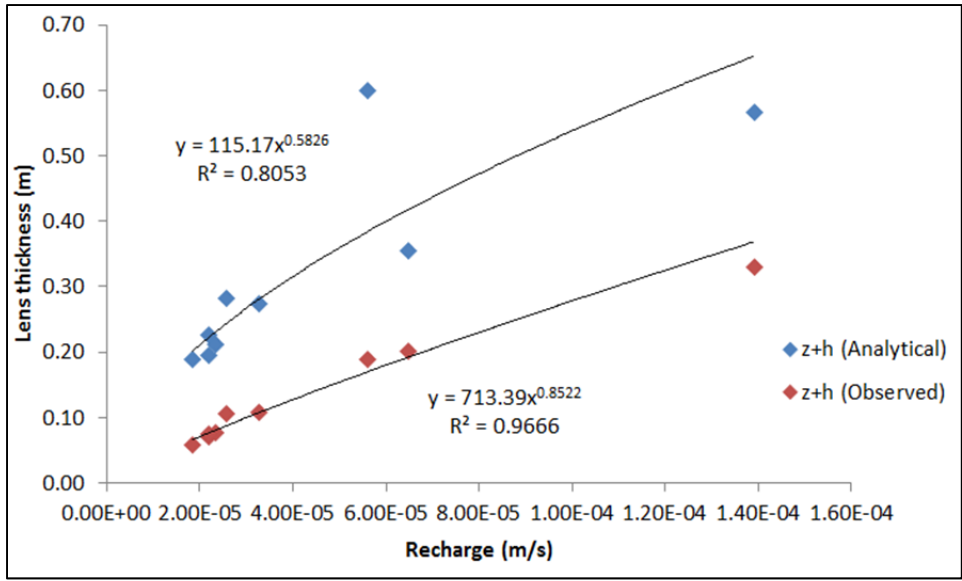


Figure 22. Lens thickness vs. recharge rate for nine simulations. Top blue data point represents simulation #3 with a high recharge area (1.04 m).

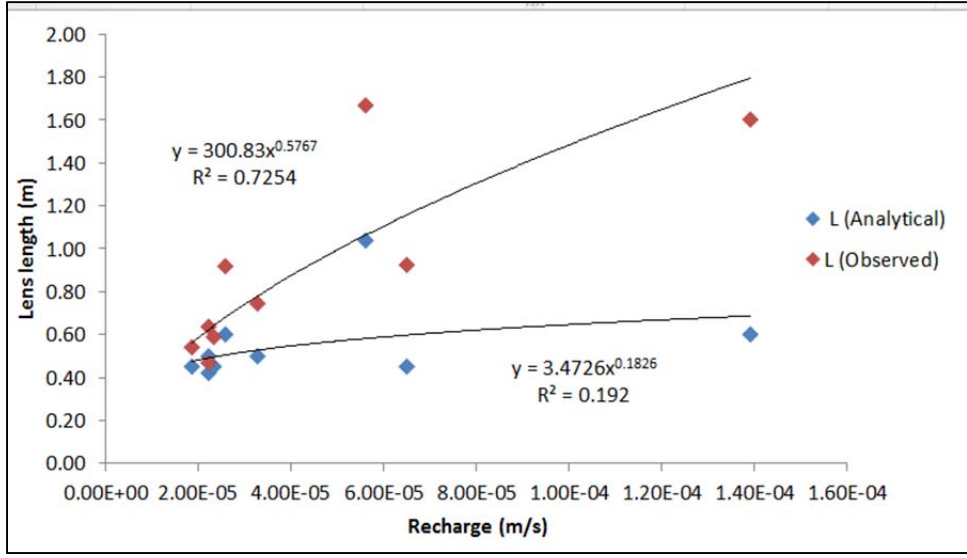


Figure 23. Lens length vs. recharge rate for nine simulations. Top red and top blue data points represent simulation #3 with high recharge area (1.04 m).

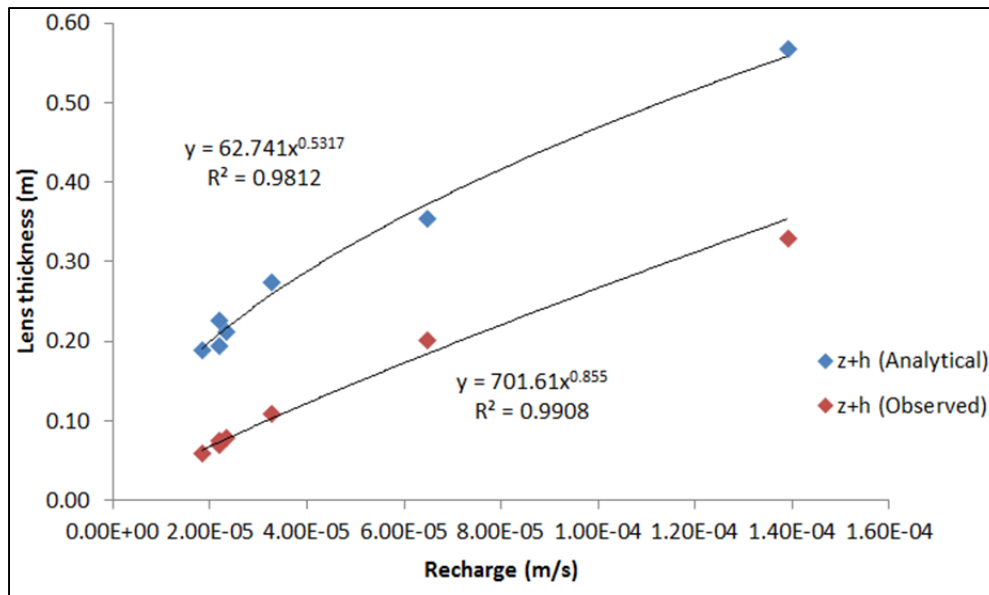


Figure 24. Lens thickness vs. recharge rate for simulations excluding simulations 3 and 4.

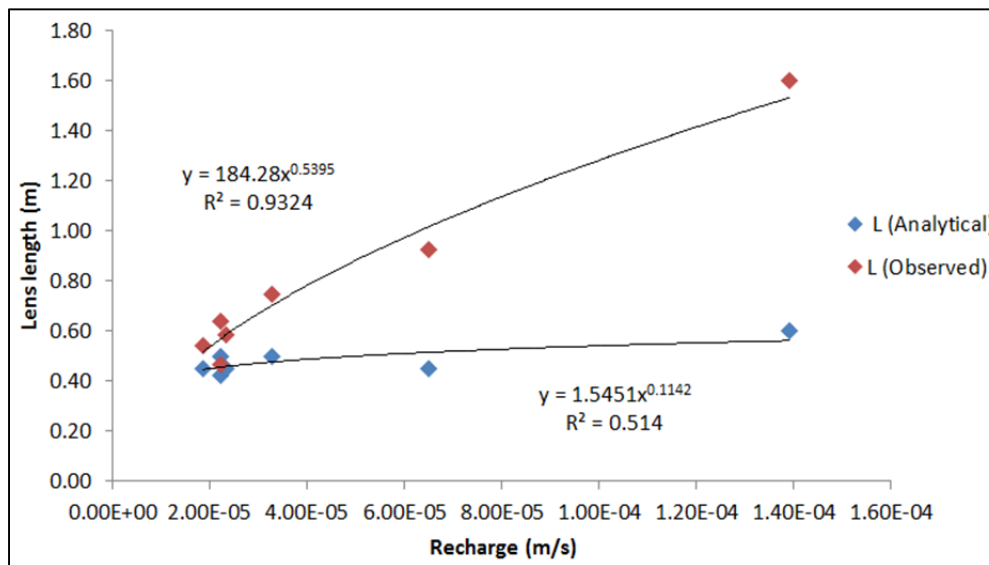


Figure 25. Lens length vs. recharge for simulations excluding simulations 3 and 4.

5.2 Recharge Effect on Observed Lens Formation

Objective: Examine the effect of recharge rate on lens formation by way of lens geometry (i.e. thickness, length)

Five simulations (6-10) were observed to analyze the effect of recharge on lens formation. A maximum lens thickness was reached during all simulations. Again, lens thickness ($z + h$) and lens length (L) were measured (Figure 26). The time required for a lens to reach maximum thickness (T_{max}) was compared to recharge rate (Table 7). All lenses reached a maximum thickness in 7440 seconds or less but always after 3600 seconds, which was when recharge halted. Results demonstrate that the time to maximum thickness is negatively correlated to recharge rate (Figure 27). As recharge rate or volume increased, the amount of time required for a lens to reach a maximum thickness decreased. The simulation with the highest volume of recharge (175 mL/min) reached a maximum thickness in the fastest time (6180 s).

In the study by Dose et al. (2014), an island lens simulation with a recharge rate of 1.152 m/d reached a maximum thickness of 15 cm after 200 minutes. The most comparable inland lens simulation was one with a recharge of 1.598 m/d, during which an inland lens reached a maximum thickness of 6 cm in 132 minutes. These results mirrored those reported when comparing the analytical and observed lenses. Inland lenses are thinner than island lenses. However, in terms of the effect of recharge rate on maximum thickness, these results show the inland lens formed more quickly when a higher recharge rate was applied, but it is also likely that other conditions (i.e. saline groundwater flow) had an effect on inland lens formation rate and maximum thickness for the simulations. Lastly, both length and thickness are positively

correlated with recharge rate. Figure 28 shows lens length is larger than lens thickness for all observed lenses at the time of maximum thickness.

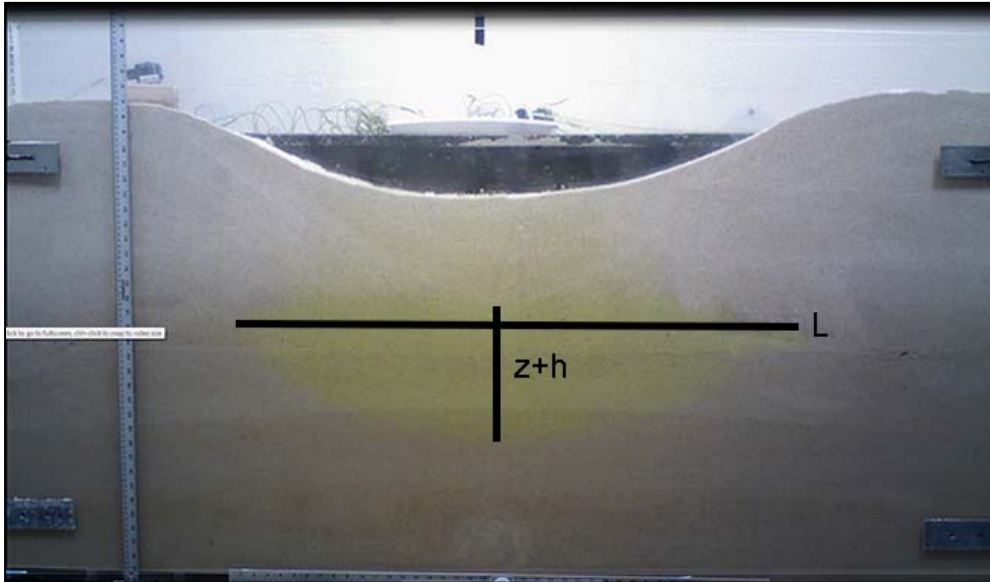


Figure 26. Simulation 8 at the time of maximum thickness (6180). Total thickness ($z+h$) and length (L) were measured.

Table 7. Recharge rates and values of time to maximum thickness for simulations 6-10.

Sim	R (ml/min)	R (m/s)	R (m/d)	R (mm/hr)	Time z+h max (s)
6	50	1.85E-05	1.60	15	7920
7	98	3.27E-05	2.82	30	6840
8	175	6.48E-05	5.60	53	6180
9	63	2.33E-05	2.02	19	6960
10	60	2.21E-05	1.92	18	7440

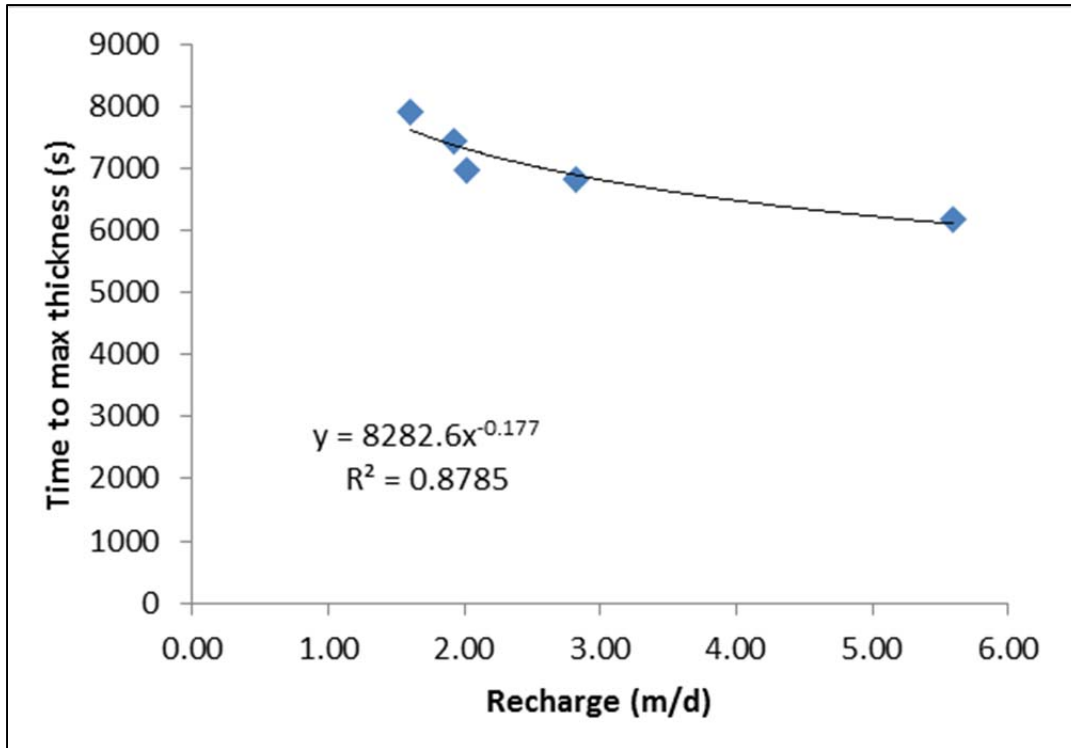


Figure 27. As recharge rate increases, the time required for a lens to reach maximum thickness decreases.

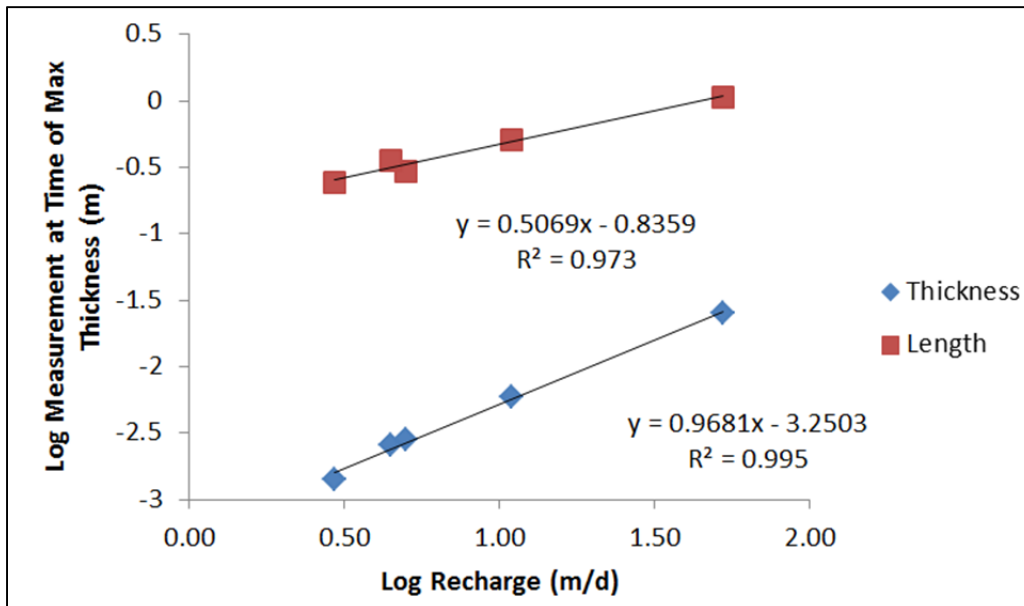


Figure 28. Length and thickness at the time of maximum thickness are both a function of recharge rate.

5.3 Recharge Effect on Degradation Rate

Objective: Analyze the effect of recharge rate on lens degradation by way of lens geometry (i.e. thickness, length)

After a simulated lens reached a maximum thickness (T_{max}), measurements of both lens length (L) and thickness ($z+h$) continued for every 3600 seconds. The lens appeared to stretch and extended laterally in the direction of the simulated gradient. It is important to note that the “up gradient” side of the lens remained beneath the recharge zone, while the thicker part of the lens migrated towards the acrylic tank wall (Figure 29). Measurements ceased at 43200 seconds, or less for simulations of larger recharge values due to deformation caused by the tank wall. For all simulations, lens length increased, while lens thickness decreased through time. Statistical analysis was performed to calculate the rate of decrease in thickness, referred to as the degradation rate for each simulation (Appendix B). Linear, power, and exponential analyses were performed. Power and exponential regressions generally fit best overall, but the exponential regression model was chosen to correct skewness only of the y-axis. Prediction values were calculated to determine the time required for the lens thickness to degrade to a value of 0.01 m or a minimum lens thickness (T_{min}) (Table 8). These values were plotted as a function of recharge to create a prediction model of degradation among various recharge values (Figure 30). Again, the exponential prediction model produced values more in line with observations. Results show the time required for a lens to degrade (T_{min}) is positively correlated with recharge rate. However, due to the exponential nature of the relationship, the rate of degradation decreases through time. For example, see Appendix C for exponential graphs of length and thickness during degradation for simulation #6.

In the study by Dose et al. (2014), an island lens degraded from a maximum thickness of 15 to 2 cm after 800 minutes with a recharge rate of 1.152 m/d. For an inland lens simulation with a recharge rate of 1.598 m/d, lens thickness degraded from 6 to 3 cm after 800 minutes. To conclude that inland lenses take longer than island lenses to degrade at this time is not clear. It is possible that the tank wall prevented the inland lens from degrading after an unknown position. Further, as mentioned in the lens formation results section, saline groundwater flow may also affect degradation rate but was not tested in these simulations.



Figure 29. Simulation showing lens degradation and lateral flow in the direction of the gradient.

Table 8. Predicted values of lens degradation for each simulation utilizing an exponential model.

Sim	Recharge (m/d)	Time (h)
6	1.60	48
7	2.82	66
8	5.60	103
9	2.02	59
10	1.92	59

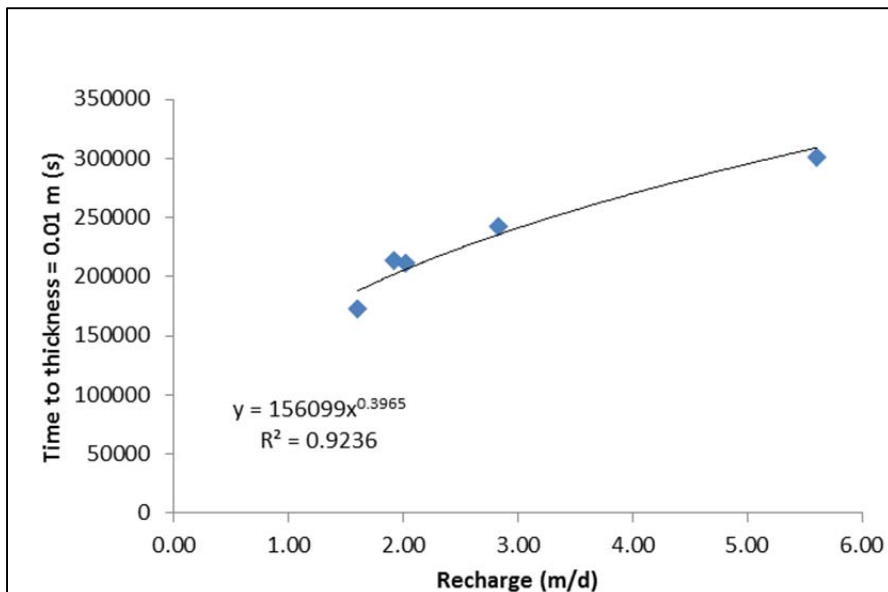


Figure 30. Prediction of lens degradation as a function of recharge rate.

CHAPTER 6

SUMMARY AND CONCLUSION

Differences between island and inland lenses create the challenge of quantifying available freshwater in regions such as northern Kuwait, where these unique resources occur. Using a physical model, this study simulated the formation and degradation of inland freshwater lenses similar to those known in northern Kuwait. Nine simulations demonstrated that inland lenses are thinner and longer than oceanic lenses and flow laterally in the direction of the gradient. On average, the analytical solutions produced lens thickness values that were 58% higher than observed inland lenses, and length values that were 59% shorter than inland lenses. When comparing inland lens simulations to island simulations by Dose et al. (2014), results demonstrated inland lenses are thinner (e.g. 6 cm) than island (e.g. 15 cm) lenses at the time of maximum thickness. However, more research is needed to determine the effective difference between island and inland lenses in terms of recharge on lens formation and degradation. When considering solely the effect of recharge rate on inland lens formation, this study confirmed that recharge rate is a controlling factor of lens formation and degradation. Recharge rates and lens formation are inversely correlated, in such that the time required for a lens to reach a maximum thickness decreases as recharge rate increases. The formation time (T_{max}) as a function of recharge for simulations 6 – 10 was calculated as:

$$T_{max} = 8282.6 * R^{-0.177}$$

Lastly, recharge rate is positively correlated with lens degradation showing that as recharge rate increases, the time required for a lens to reach a minimum thickness (T_{min}) also increases. The degradation rate as a function of recharge for simulations 6 – 10 was calculated as:

$$T_{min} = 156099 * R^{0.3965}$$

While these rates cannot be applied directly to the inland lenses of northern Kuwait, understanding these relationships lays the groundwork to improve estimates in hydrologic models. Simulated lenses flow freely in the direction of the gradient in a tongue shape much like a contaminant or light non-aqueous phase liquid. Accounting for this movement, also referred to as lens degradation, is imperative when estimating the amount of freshwater directly beneath the depression center through time. In addition, lens formation occurred in simulations testing recharge rates as low as 16 mm/hr indicating the likelihood for depression focused recharge in Kuwait to be more spatially abundant and frequent due to high infiltration rates in the surface sediments and other conditions (e.g. topography, climate) that promote lens formation and sustainability. In addition, implications suggest that depression focused recharge occurs across the Arabian Peninsula in more locations than previously believed, as well as other dryland environments on Earth with similar conditions. Results provide support for in-situ field research utilizing geophysical and other hydrological techniques to verify proposed locations.

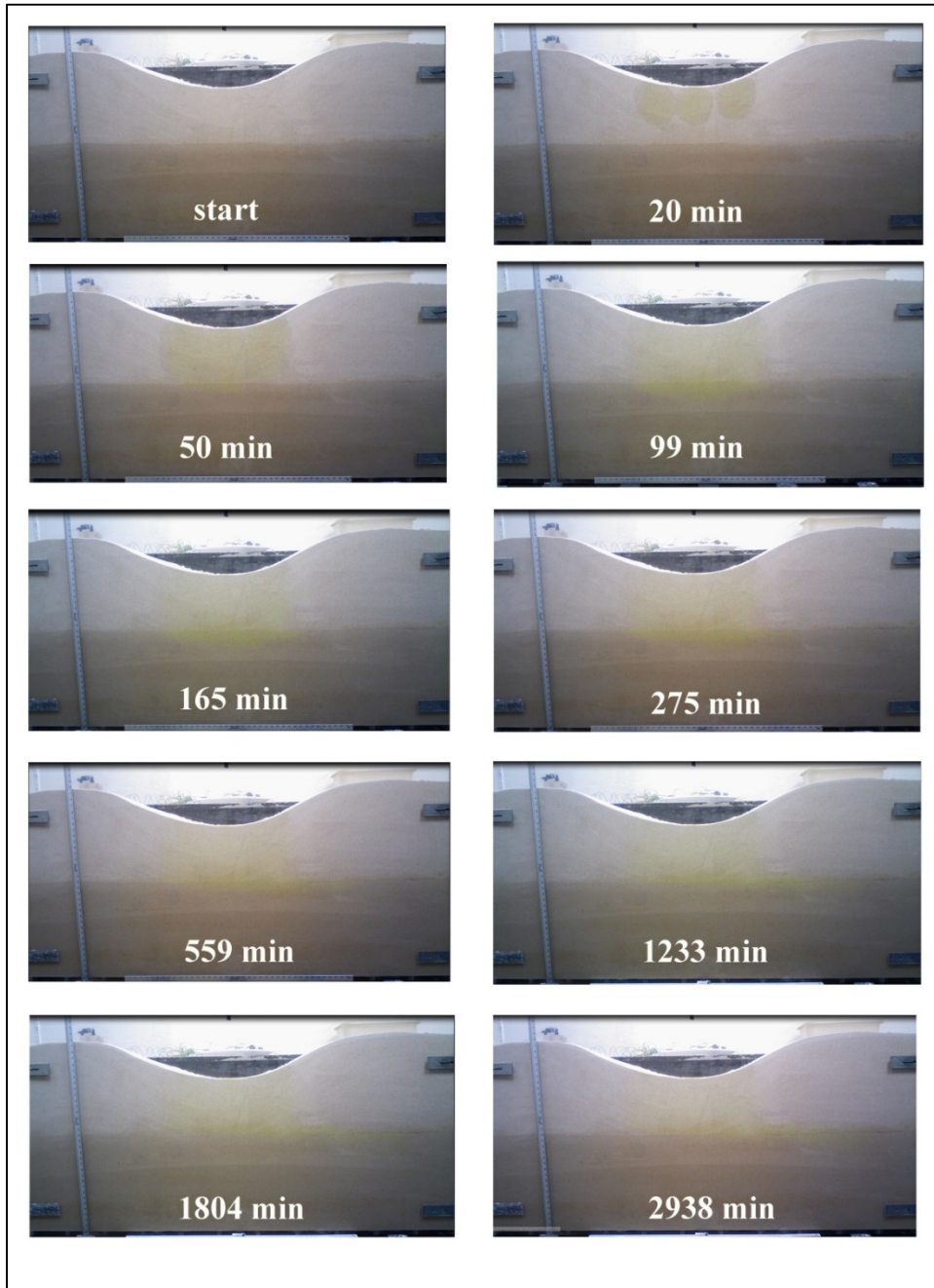
Future research is required to fully characterize the relationship between recharge (R), lens thickness ($z+h$), length (L), hydraulic conductivity (K), and groundwater flow (Q). Further, it is important to note that recharge area also appears to play a role in lens length due to observations made during practice simulations. These relationships can be explored with a physical model like the one used in this study, but one must keep in mind its limitations. The hydraulic conductivity of Kuwait's subsurface is extremely heterogeneous. Lens shape is likely much less perfect than

the idealized shape assumed in this study. Scaling, recharge distribution, tidal forcing, and temperature variability are all examples that present challenges for the physical model. While, this study demonstrated that analytical solutions created for oceanic island lenses cannot characterize inland lenses due differing boundary conditions, the physical model can assist in analytically solving parameter relationships, upon which subsequent volume calculations for a circular depression can be calculated to determine freshwater availability. Further, volume calculations such as the amount of water held in the unsaturated zone and minimum amount of rainfall to create an inland lens could also be tested with the physical model. Since inland freshwater lenses are the only source of renewable freshwater in Kuwait, the estimation of availability is a useful tool in the management and development of water resources in arid environments with similar geologic and hydrologic settings. Understanding the relationship of recharge rate on lens formation and degradation serves to protect current reserves and reinforce the usefulness of new technologies like artificial recharge, both of which are important for sustainable practices.

APPENDICES

Appendix A

Time-lapse photos of simulation 6 showing lens development and degradation through time.



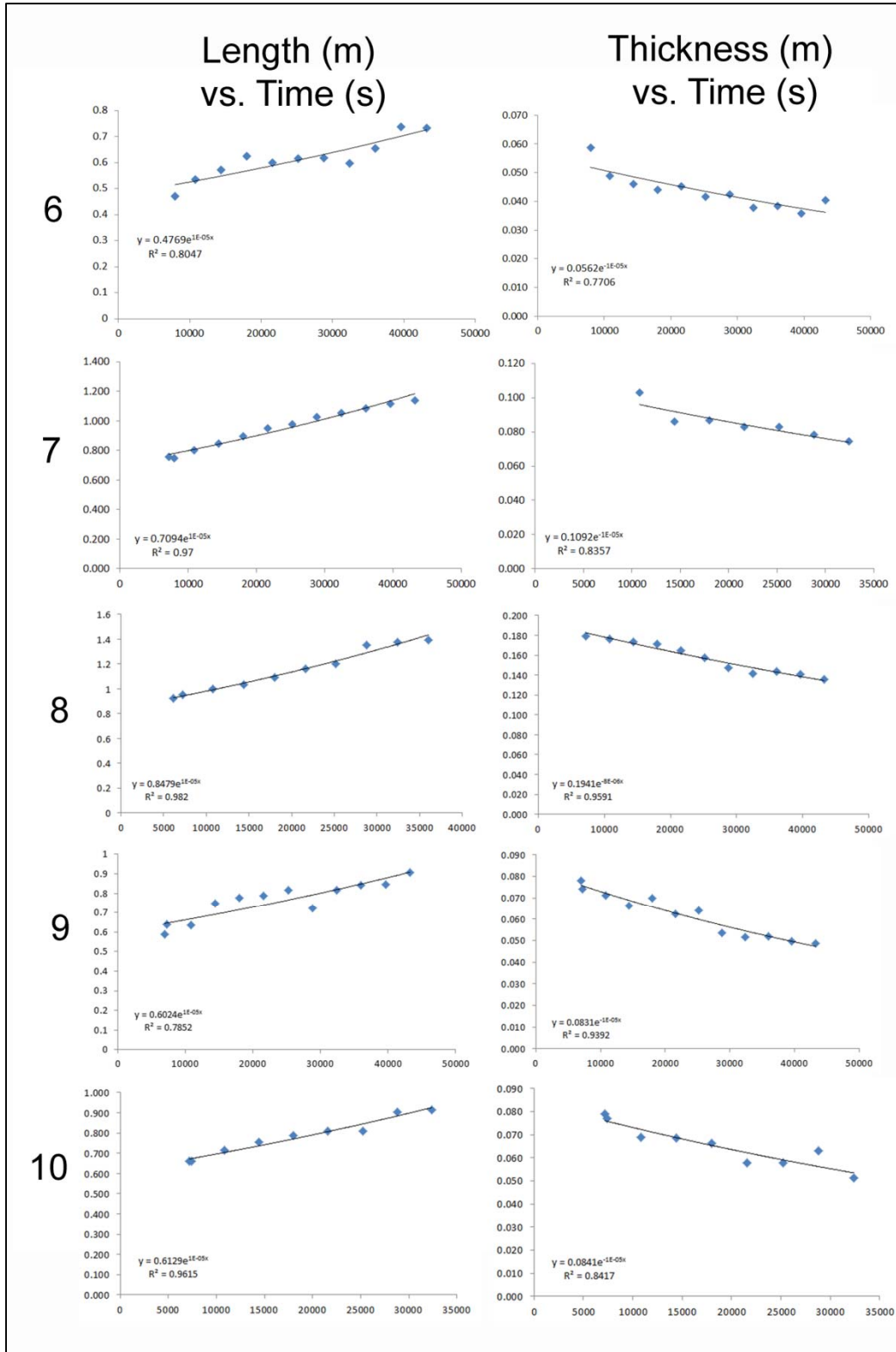
Appendix B

Lens thickness and length statistics including linear, power, and exponential models for simulations 6-10 for lens degradation analyses.

Simulation	Regression	Slope	Intercept	R-squared	Variable
6	Log-log	0.2126000	-1.1391	0.8341	Length
6	Linear	0.0000060	0.4650	0.8142	Length
6	Log-Linear	0.0000040	-0.3216	0.0470	Length
6	Log-log	-0.2322000	-0.3524	0.8681	Thickness
6	Log-Linear	-0.0000040	-1.2503	0.7706	Thickness
6	Linear	-0.0000005	0.0555	0.7389	Thickness
7	Log-log	0.2400000	2.4432	0.9912	Length
7	Linear	0.0000100	0.6900	0.9900	Length
7	Log-Linear	0.0000100	0.3434	0.9700	Length
7	Log-log	-0.2680000	0.1666	0.9361	Thickness
7	Log-Linear	-0.0000100	-2.1780	0.9156	Thickness
7	Linear	-0.0000010	0.1104	0.8973	Thickness
8	Log-Linear	0.0000060	-0.0717	0.9820	Length
8	Linear	0.0000200	0.8117	0.9762	Length
8	Log-log	0.2401000	-0.9614	0.9285	Length
8	Log-log	-0.1719000	-0.0548	0.9227	Thickness
8	Linear	-0.0000020	0.2000	0.9053	Thickness
8	Log-Linear	-0.0000040	-0.6932	0.8977	Thickness
9	Log-log	0.1950000	-0.9614	0.8564	Length
9	Linear	0.0000070	0.5939	0.8054	Length
9	Log-Linear	0.0000040	-0.2201	0.7852	Length
9	Log-Linear	-0.0000060	-1.0802	0.9397	Thickness
9	Linear	-0.0000008	0.0807	0.9341	Thickness
9	Log-log	-0.2488000	-0.1434	0.8874	Thickness
10	Linear	0.0000100	0.5970	0.9783	Length
10	Log-Linear	0.0000060	-0.21216	0.9724	Length
10	Log-log	0.2085000	-0.9884	0.9691	Length
10	Linear	-0.0000009	0.0823	0.8452	Thickness
10	Log-Linear	-6.00E-06	-0.0751	0.8417	Thickness
10	Log-log	-0.2299000	-0.2193	0.8496	Thickness

Appendix C

Lens length (left) and thickness (right) regressions for simulations 6-10 for degradation analyses.



REFERENCES

- Al-Awadhi, J.M., Al-Dousari, A.M., Khalaf, F.I., 2014. Influence of land degradation on the local rate of dust fallout in Kuwait. *Atmospheric and Climate Sciences* 2014.
- Al-Dabi, H., Koch, M., Al-Sarawi, M., El-Baz, F., 1997. Evolution of sand dune patterns in space and time in north-western Kuwait using Landsat images. *Journal of Arid Environments* 36, 15-24.
- Al-Rashed, M., Sherif, M., 2000. Water Resources in the GCC Countries: An Overview. *Water Resources Management* 14, 59-75.
- Al-Ruwaih, F., Hadi, K., 2005. Water quality trends and management of fresh groundwater at Rawdhatain, Kuwait. *Editorial Advisory Board* e 11, 423-437.
- Al-Ruwaih, F., Sayed, S., Al-Rashed, M., 1998. Geological controls on water quality in arid Kuwait. *Journal of Arid Environments* 38, 187-204.
- Al-Sarawi, M., 1995. Surface geomorphology of Kuwait. *GeoJournal* 35, 493-503.
- Al-Sulaimi, J., Khalaf, F.J., Mukhopadhyay, A., 1997. Geomorphological analysis of paleo drainage systems and their environmental implications in the desert of Kuwait. *Environmental Geology* 29, 94-111.
- Al-Sulaimi, J., Mukhopadhyay, A., 2000. An overview of the surface and near-surface geology, geomorphology and natural resources of Kuwait. *Earth-Science Reviews* 50, 227-267.
- Al-Sulaimi, J.S., 1988. Calcrete and near-surface geology of Kuwait City and suburbs, Kuwait, Arabian Gulf. *Sedimentary Geology* 54, 331-345.
- Al-Sulaimi, J.S., El-Rabaa, S.M., 1994. Morphological and morphostructural features of Kuwait. *Geomorphology* 11, 151-167.
- Alsharhan, A.S., Rizk, Z.A., Nairn, A.E.M., Bakhit, D.W., Alhajari, S.A., 2001a. Chapter 3 - Geology of the Arabian Peninsula and Gulf, In: Alhajari, A.S.A.A.R.E.M.N.W.B.A. (Ed.), *Hydrogeology of an Arid Region: The Arabian Gulf and Adjoining Areas*. Elsevier Science B.V., Amsterdam, pp. 55-77.
- Alsharhan, A.S., Rizk, Z.A., Nairn, A.E.M., Bakhit, D.W., Alhajari, S.A., 2001b. Chapter 4 - Aquifer and aquiclude systems, In: Alhajari, A.S.A.A.R.E.M.N.W.B.A. (Ed.), *Hydrogeology of an Arid Region: The Arabian Gulf and Adjoining Areas*. Elsevier Science B.V., Amsterdam, pp. 79-99.

- Anderson, E., 2013. Middle East: Geography and Geopolitics. Routledge.
- Baydon-Ghyben, 1898. Nota in verband met de voorgenomen putboring nabil Amsterdam'Tijdschr. K. Inst. Ing., The Hague 27, 1888-1889.
- Bear, J., 1972. Dynamics of fluids in porous media. Courier Corporation.
- Becker, M.W., 2006. Potential for satellite remote sensing of ground water. Ground water 44, 306-318.
- Bergstrom, R.E., Aten, R.E., 1965. Natural recharge and localization of fresh ground water in Kuwait. Journal of Hydrology 2, 213-231.
- Carol, E., Kruse, E., Roig, A., 2010. Groundwater travel time in the freshwater lenses of Samborombón Bay, Argentina. Hydrological sciences journal 55, 754-762.
- Chesnaux, R., Allen, D., 2008. Groundwater travel times for unconfined island aquifers bounded by freshwater or seawater. Hydrogeology Journal 16, 437-445.
- Climatemps, 2016. Rainfall and Temperature in Kuwait City. Climatemps.com <http://www.climatemps.com/>.
- Dose, E.J., Stoeckl, L., Houben, G.J., Vacher, H.L., Vassolo, S., Dietrich, J., Himmelsbach, T., 2014. Experiments and modeling of freshwater lenses in layered aquifers: Steady state interface geometry. Journal of Hydrology 509, 621-630.
- Eeman, S., Leijnse, A., Raats, P.A.C., van der Zee, S.E.A.T.M., 2011. Analysis of the thickness of a fresh water lens and of the transition zone between this lens and upwelling saline water. Advances in Water Resources 34, 291-302.
- Eeman, S., Zee, S.v.d., Leijnse, A., De Louw, P., Maas, C., 2012. Response to recharge variation of thin rainwater lenses and their mixing zone with underlying saline groundwater. Hydrology and Earth System Sciences 16, 3535-3549.
- Ergun, H., 1969. Reconnaissance soil survey. Report to the Government of Kuwait. FAO/KU/TF 17. Mimeo.
- Fadlelmawla, A., Hadi, K., Zouari, K., Kulkarni, K., 2008. Hydrogeochemical investigations of recharge and subsequent salinization processes at Al-Raudhatain depression in Kuwait/Analyses hydrogéochimiques de la recharge et des processus associés de salinisation dans la dépression de Al-Raudhatain au Koweit. Hydrological sciences journal 53, 204-223.
- Fetter, C., 1972. Position of the saline water interface beneath oceanic islands. Water Resources Research 8, 1307-1315.

- Glover, R., 1959. The pattern of fresh-water flow in a coastal aquifer. *Journal of Geophysical Research* 64, 457-459.
- Grealish, G., Omar, S., Quinn, M., 1998. Affected area soil survey—assessing damage magnitude and recovery of the terrestrial eco-system—follow-up of natural and induced desert recovery. Kuwait Institute for Scientific Research, Report No FA C 15.
- Hamoda, M.F., 2001. Desalination and water resource management in Kuwait. *Desalination* 138, 385-393.
- Henry, H.R., 1964. Interfaces between salt water and fresh water in coastal aquifers. US Geological Survey Water-Supply Paper, C35-70.
- Herzberg, D., 1901. Die wasserversorgung einiger nordseebäder.
- Himida, I.H., 1981. Groundwater in Kuwait and the Environmental Factors Affecting its Quality, In: W. van Duijvenbooden, P.G., Lelyveld, H.v. (Eds.), *Studies in Environmental Science*. Elsevier, pp. 121-124.
- Houben, G., Noell, U., Vassolo, S., Grisseman, C., Geyh, M., Stadler, S., Dose, E.J., Vera, S., 2014. The freshwater lens of Benjamín Aceval, Chaco, Paraguay: a terrestrial analogue of an oceanic island lens. *Hydrogeology journal* 22, 1935-1952.
- Khalaf, F.I., Al-Ajmi, D., 1993. Aeolian processes and sand encroachment problems in Kuwait. *Geomorphology* 6, 111-134.
- Kottek, M., Grieser, J., Beck, C., Rudolf, B., Rubel, F., 2006. World map of the Köppen-Geiger climate classification updated. *Meteorologische Zeitschrift* 15, 259-263.
- Kwarteng, A.Y., Al-Ajmi, D., 1996. Using Landsat Thematic Mapper data to detect and map vegetation changes in Kuwait. *International archives of Photogrammetry and Remote sensing* 31, 398-405.
- Kwarteng, A.Y., Viswanathan, M.N., Al-Senafy, M.N., Rashid, T., 2000. Formation of fresh ground-water lenses in northern Kuwait. *Journal of Arid Environments* 46, 137-155.
- Lezzaik, K., Milewski, A., 2015. A Quantitative Assessment of Groundwater Resources in the Middle East and North Africa Region *Journal of Arid Environments*.
- Lissey, A., 1971. Depression-focused transient groundwater flow patterns in Manitoba. *Geological Association of Canada Special Paper* 9, 333-341.
- Marcella, M.P., Eltahir, E.A., 2008. The hydroclimatology of Kuwait: explaining the variability of rainfall at seasonal and interannual time scales. *Journal of hydrometeorology* 9, 1095-1105.

- Meixner, T., Manning, A.H., Stonestrom, D.A., Allen, D.M., Ajami, H., Blasch, K.W., Brookfield, A.E., Castro, C.L., Clark, J.F., Gochis, D.J., 2016. Implications of projected climate change for groundwater recharge in the western United States. *Journal of Hydrology* 534, 124-138.
- Membery, D., 1983. Low level wind profiles during the Gulf Shamal. *Weather* 38, 18-24.
- Milewski, A., Sultan, M., Al-Dousari, A., Yan, E., 2014. Geologic and hydrologic settings for development of freshwater lenses in arid lands. *Hydrological Processes* 28, 3185-3194.
- Milton, D.I., 1968. *Geology of the Arabian Peninsula; Kuwait*. U. S. Geological Survey : Reston, VA, United States, United States.
- Misak, R.F., Khalaf, F.I., Omar, S.A., 2013. *Managing the Hazards of Drought and Shifting Sands in Dry Lands: The Case Study of Kuwait, Developments in Soil Classification, Land Use Planning and Policy Implications*. Springer, pp. 703-729.
- Omar, S., 1982. Artificial recharge into the Kuwait Group at Ar-Rawdhatain. M. Sc. Thesis, Loughborough University of Technology. Water quality trends and management of fresh groundwater 437.
- Omar, S., Al-Yaqubi, A., Senay, Y., 1981. Geology and groundwater hydrology of the State of Kuwait. *Journal of the Gulf and Arabian Peninsula Studies* 1, 5-67.
- Parson's Corporation, L.A.C., 1961. Fresh ground-water resources, Rawdatain area, Kuwait : final report. The Parson's Corporation Los Angeles.
- Parson's Corporation, L.A.C., 1964. Ground-water resources of Kuwait.
- Pennink, J.M.K., 1915. *Groundwater Stroombanen (Flowpaths)*. Stadsdrukkery Amsterdam.
- Rotz, R., Milewski, A., 2014. Understanding Hydrologic Alterations and Physiographic Changes in Kuwait from Prolonged Drought and Climate Change, 2014 GSA Annual Meeting in Vancouver, British Columbia.
- Sayed, S.A.S., Saeedy, H.S., Székely, F., 1992. Hydraulic parameters of a multilayered aquifer system in Kuwait City. *Journal of Hydrology* 130, 49-70.
- Scanlon, B.R., Levitt, D.G., Reedy, R.C., Keese, K.E., Sully, M.J., 2005. Ecological controls on water-cycle response to climate variability in deserts. *Proceedings of the National Academy of Sciences* 102, 6033-6038.
- Senay, Y., 1977. Groundwater resources and artificial recharge in Rawdhatain water field. Ministry of Electricity and Water, Kuwait 35.

- Stoeckl, L., Houben, G., 2012. Flow dynamics and age stratification of freshwater lenses: Experiments and modeling. *Journal of Hydrology* 458–459, 9-15.
- Stuyfzand, P.J., Bruggeman, G., 1994. Analytical approximations for fresh water lenses in coastal dunes, Proc. 13th Salt Water Intrusion Meeting (SWIM), Cagliari, Italy, pp. 15-33.
- Taylor, R.G., Scanlon, B., Döll, P., Rodell, M., Van Beek, R., Wada, Y., Longuevergne, L., Leblanc, M., Famiglietti, J.S., Edmunds, M., 2013. Ground water and climate change. *Nature Climate Change* 3, 322-329.
- UN-ESCWA, B., 2013. Inventory of shared water resources in Western Asia: Chapter 6 Jordan River Basin. United Nations Economic and Social Commission for Western Asia. Federal Institute for Geosciences and Natural Resources, Beirut.
- University of East Anglia, C.R.U., 2016. Average monthly temperature and rainfall for Kuwait from 1900-2012, Climate Change Knowledge Portal. The World Bank Group, <http://sdwebx.worldbank.org/>.
- Vacher, H., 1988. Dupuit-Ghyben-Herzberg analysis of strip-island lenses. *Geological Society of America Bulletin* 100, 580-591.
- Van Der Veer, P., 1977. Analytical solution for steady interface flow in a coastal aquifer involving a phreatic surface with precipitation. *Journal of Hydrology* 34, 1-11.
- Viswanathan, M.N., 1997. Assessment of long-term pollution potential of the groundwater of Raudhatain-Umm Al-Aish Area, Phase II / M. N. Viswanathan, Hydrology Department, Water Resources Division. Kuwait : KISR.
- Werner, A.D., Jacobsen, P.E., Morgan, L.K., 2013. Understanding seawater intrusion. Flinders Academic Commons.
- Werner, A.D., Laattoe, T., 2016. Terrestrial freshwater lenses in stable riverine settings: Occurrence and controlling factors. *Water Resources Research*.
- Zhao, J., Wen, Z., Shu, L., Zhen, L., Zhou, C., Liu, L., 2009. A laboratory model of the evolution of an island freshwater lens. IAHS-AISH Publication 330, 154-161.